

Review

# Catalysis for CO<sub>2</sub> Hydrogenation—What We Have Learned/Should Learn from the Hydrogenation of Syngas to Methanol

Zixu Yang <sup>1</sup>, Derun Guo <sup>1</sup>, Shengbin Dong <sup>1</sup>, Jiayi Wu <sup>1</sup>, Minghui Zhu <sup>1,\*</sup>, Yi-Fan Han <sup>1,2,\*</sup> and Zhong-Wen Liu <sup>3,\*</sup>

<sup>1</sup> State Key Laboratory of Chemical Engineering, East China University of Science and Technology, Shanghai 200237, China; zixu.yang@ecust.edu.cn (Z.Y.); 17318588105@163.com (D.G.); y30220007@mail.ecust.edu.cn (S.D.); y11220015@mail.ecust.edu.cn (J.W.)

<sup>2</sup> Engineering Research Center of Advanced Functional Material Manufacturing of Ministry of Education, Zhengzhou University, Zhengzhou 450001, China

<sup>3</sup> Key Laboratory of Syngas Conversion of Shaanxi Province, School of Chemistry & Chemical Engineering, Shaanxi Normal University, Xi'an 710119, China

\* Correspondence: minghui.zhu@ecust.edu.cn (M.Z.); yifanhan@ecust.edu.cn (Y.-F.H.); zwliu@snnu.edu.cn (Z.-W.L.); Tel.: +86-021-64251928 (Y.-F.H.); Fax: +86-021-64253528 (Y.-F.H.)

**Abstract:** This short review provides an in-depth analysis of the achievements and further developments of the catalytic hydrogenation of carbon dioxide (CO<sub>2</sub>) to methanol from those that are worth learning about based on the transformation of syngas into methanol. We begin by exploring the environmental and energy-related implications of utilizing CO<sub>2</sub> as a feedstock for methanol production by emphasizing its potential to mitigate greenhouse gas emissions and facilitate renewable energy integration. Then, different catalytic formulations focusing on precious metals, copper-based catalysts, and metal oxides are summarized, and insights into their advantages and limitations in the aspects of catalytic activity, selectivity, and stability are discussed. Precious metal catalysts, such as platinum and iridium, exhibit high activity but are cost-prohibitive, while copper-based catalysts present a promising and cost-effective alternative. Metal oxides are considered for their unique properties in CO<sub>2</sub> activation. Mechanistic insights into reaction pathways are explored, with a particular emphasis on copper-based catalysts. Moreover, the complex steps involved in CO<sub>2</sub> hydrogenation to methanol are discussed to shed light on the key intermediates and active sites responsible for catalysis, which is crucial for catalyst design and optimization. Finally, we stress the importance of ongoing research and development efforts to enhance catalyst efficiency, mechanistic comprehension, and process optimization. This review serves as a valuable resource for researchers, engineers, and policymakers working toward a more sustainable and carbon-neutral energy future. By harnessing CO<sub>2</sub> as a carbon feedstock for methanol synthesis, we have the potential to address environmental concerns and advance the utilization of renewable energy sources, further contributing to the transition to a cleaner and more sustainable energy landscape.

**Keywords:** CO<sub>2</sub>/CO hydrogenation; methanol synthesis; metal nanoparticles; metal–support interaction; reaction mechanism



**Citation:** Yang, Z.; Guo, D.; Dong, S.; Wu, J.; Zhu, M.; Han, Y.-F.; Liu, Z.-W. Catalysis for CO<sub>2</sub> Hydrogenation—What We Have Learned/Should Learn from the Hydrogenation of Syngas to Methanol. *Catalysts* **2023**, *13*, 1452. <https://doi.org/10.3390/catal13111452>

Academic Editor: Maria A. Goula

Received: 27 October 2023

Revised: 13 November 2023

Accepted: 15 November 2023

Published: 20 November 2023



**Copyright:** © 2023 by the authors. Licensee MDPI, Basel, Switzerland. This article is an open access article distributed under the terms and conditions of the Creative Commons Attribution (CC BY) license (<https://creativecommons.org/licenses/by/4.0/>).

## 1. Introduction

Since the Industrial Revolution, the intensification of anthropogenic activities has led to a marked increase in energy consumption, primarily driven by the combustion of fossil fuels. This has resulted in a significant rise in atmospheric carbon dioxide (CO<sub>2</sub>) concentrations, contributing to notable environmental challenges, such as global warming, ocean acidification, and terrestrial desertification. To address these issues, carbon capture, utilization, and storage (CCUS) has been identified as a key technological intervention. Central to CCUS is the strategy of converting captured CO<sub>2</sub> into economically valuable

products rather than simply storing it [1,2]. Within this framework, methanol emerges as a prominent candidate for both a chemical building block and an energy carrier. Its versatile nature allows for diverse applications in organic synthesis, pharmaceuticals, coatings, and the automotive and defense industries. Notably, when derived from CO<sub>2</sub>, methanol offers a renewable alternative to traditional production methods that rely on fossil fuels [3,4]. The catalytic hydrogenation of CO<sub>2</sub>, especially when coupled with hydrogen from renewable sources, is gaining traction as a sustainable method of methanol production. This approach underscores the dual objectives of CCUS, i.e., addressing environmental concerns while facilitating sustainable industrial practices.

Carbon dioxide is the ultimate oxidation state of carbon-containing compounds, with a characteristically stable molecular structure, and has been traditionally perceived as an inert molecule under typical conditions. This inherent chemical stability has presented challenges in its chemical utilization. Achieving the activation of this inert chemical typically requires elevated temperatures and pressures to surmount the kinetic barriers (C=O bond energy is approximately 750 kJ·mol<sup>-1</sup>). The introduction of hydrogen (H<sub>2</sub>) to this landscape has been transformative. Recognized for its high-energy molecular nature and wide-ranging sources in the chemical industry, H<sub>2</sub> has emerged as the prime candidate for CO<sub>2</sub> activation. This synergy between CO<sub>2</sub> and H<sub>2</sub> is not merely a serendipitous observation. In fact, it finds resonance in the methanol economy proposed by Nobel laureate George Olah [5,6]. In this vision, CO<sub>2</sub> hydrogenation to methanol and its derivatives holds a central role, which bridges the gap between carbon emissions and sustainable fuel alternatives (Figure 1).

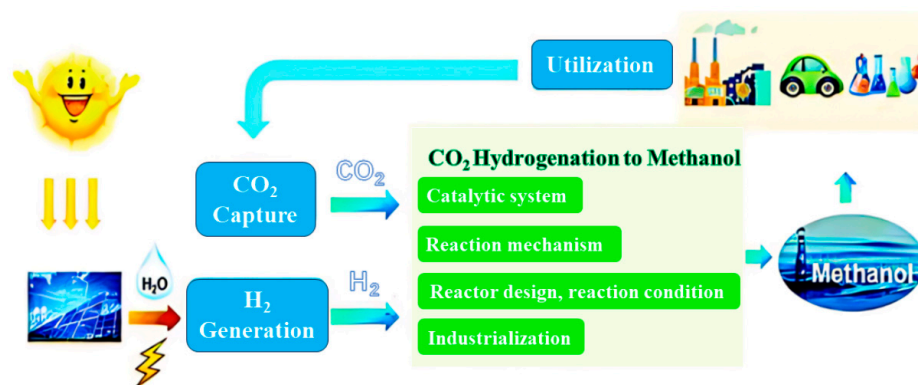
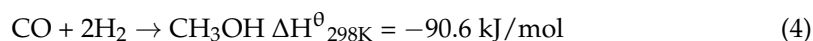
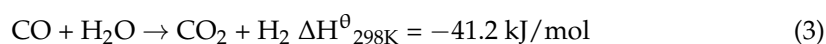
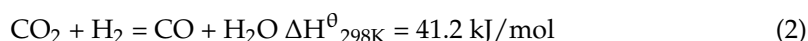
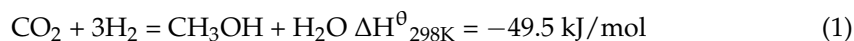


**Figure 1.** Heterogeneous hydrogenation of CO<sub>2</sub> to methanol. Reproduced with permission from ref. [7]. Copyright 2020, the Royal Society of Chemistry.

Focusing on the chemical intricacies of the process, CO<sub>2</sub> hydrogenation primarily culminates in two outcomes, i.e., the formation of methanol or carbon monoxide (CO). These transformations are defined by the following reactions:



Extrapolating from these equations, the hydrogenation of CO<sub>2</sub> to methanol emerges as an exothermic reaction with decreased molecular volume. These thermodynamic insights provide a roadmap for optimization; conditions involving low temperatures and high pressures favor methanol production, whereas elevated temperatures are inclined toward CO formation [8] (Figure 2).

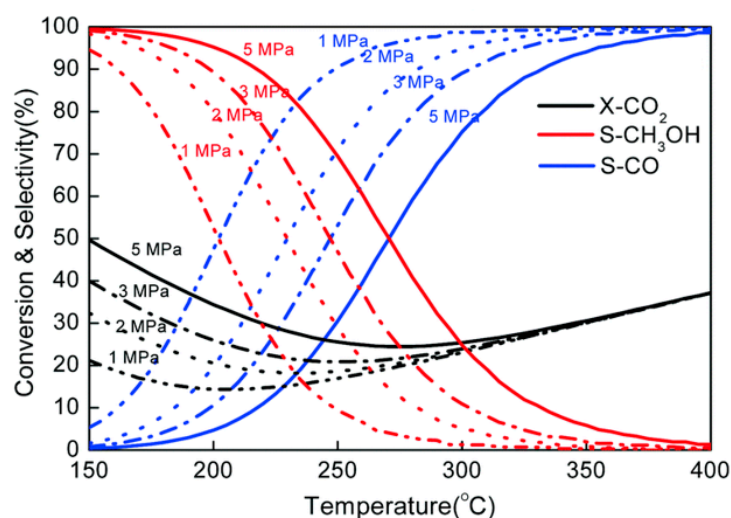


**Figure 2.** Equilibrium conversion–selectivity values of the  $\text{CO}_2$  hydrogenation reaction at various pressures. Reproduced with permission from ref. [7]. Copyright 2020, the Royal Society of Chemistry.

Historically, this field has witnessed steady evolution. Tracing back to the 1940s, foundational studies by Ipatieff et al. [9] marked the inception of research into  $\text{CO}_2$ 's viability as a carbon source alternative to CO. Fast forward to the 1960s, and technological shifts were palpable. With the advent of the high-selectivity  $\text{Cu-ZnO-Al}_2\text{O}_3$  catalysts developed by Imperial Chemical Industries (ICI) and a pivot in raw materials from coal to naphtha/natural gas, there was a marked upswing in the catalytic activity. The subsequent decades were marked by continued innovations, with companies such as Topsoe, Lurgi, and Süd-Chemie contributing significant findings, cementing our understanding of these reactions and their thermodynamic preferences [10]. In the current landscape, it is evident that, while challenges remain, the insights from previous studies and the potential economic and environmental benefits of the process underscore the relevance and promise of  $\text{CO}_2$  hydrogenation to methanol.

Syngas to methanol represents one of the most important coal-to-chemical processes in China. Technically, syngas with a small portion of  $\text{CO}_2$  at ~5 vol% is indispensable in achieving a reasonably higher methanol formation rate over commercial catalysts. Mechanistically, extensive efforts have been dedicated to unravelling the reaction mechanism, resulting in various proposed explanations. These endeavors have significantly contributed to a profound comprehension of the elementary steps occurring across catalyst surfaces [11–14]. However, the mechanistic function of  $\text{CO}_2$  is still far from clear [15–18]. Taking the involved reactions into account, they are very similar to  $\text{CO}_2$  hydrogenation to methanol (Equations (1), (2), and (4)) and syngas to methanol (Equations (1), (3), and (4)). Moreover, the reported catalysts for  $\text{CO}_2$  hydrogenation to methanol are overwhelmingly derived from those of syngas to methanol. Taking these facts into account, in this mini-review, achievements related to methanol synthesis from either CO or  $\text{CO}_2$  hydrogenation are discussed, and emphasis is placed on further developments regarding  $\text{CO}_2$  hydrogenation to methanol based on the knowledge of CO hydrogenation to methanol.

## 2. Current Status of Syngas to Methanol

The realm of  $\text{CO}_2$  hydrogenation to methanol is dominated by three primary categories of catalysts, i.e., transition metal catalysts, especially Cu-based catalysts; precious metal catalysts; and metal oxide catalysts. Cu-based catalysts are widely acknowledged for their exceptional catalytic activity, chiefly represented by formulations such as  $\text{Cu-ZnO-Al}_2\text{O}_3$ . Supported precious metal catalysts have foundational examples like  $\text{Pd/Ga}_2\text{O}_3$  and  $\text{Pd/SiO}_2$ , with modern research gravitating toward Rh-based variants. The metal oxide catalysts, either composed of single metal oxides or bimetallic solid solutions, are renowned for their structural stability at elevated temperatures. A detailed comparison of the catalytic

properties of some commonly used methanol synthesis catalysts is provided in Table 1. A consensus has been established highlighting Cu-based catalysts as exhibiting the highest methanol formation rate, with an excellent selectivity of approximately 80%. However, attempting to further enhance selectivity may come at the cost of a reduced formation rate. In contrast, precious metal catalysts achieve higher selectivity at lower temperatures than Cu-based catalysts, albeit at a lower rate. Metal oxide catalysts, such as  $\text{In}_2\text{O}_3$ ,  $\text{ZnO}$ , and  $\text{Ga}_2\text{O}_3$ , consistently demonstrate excellent methanol selectivity, exceeding 90%, albeit under low conversion rates. Notably, their operating temperatures are considerably higher compared with Cu-based and precious metal catalysts.

**Table 1.** Methanol synthesis performance of various metal catalysts.

Catalysts	Temperature (°C)	H <sub>2</sub> : CO <sub>2</sub> Ratio	Pressure (MPa)	CO <sub>2</sub> Conversion (%)	MeOH Selectivity (%)	Yield (g <sub>MeOH</sub> ·kg <sub>cat</sub> <sup>-1</sup> ·h <sup>-1</sup> )
Cu/ $\gamma$ -Al <sub>2</sub> O <sub>3</sub> [19]	200	3.8	10	N/A	45	N/A
Cu-K/ $\gamma$ -Al <sub>2</sub> O <sub>3</sub> [19]	200	3.8	10	N/A	5	N/A
Cu-Ba/ $\gamma$ -Al <sub>2</sub> O <sub>3</sub> [19]	200	3.8	10	N/A	63	N/A
Ga-Cu-Zn/ZrO <sub>2</sub> [20]	250	3	4	18	69	512
Cu-Zn/SiO <sub>2</sub> [21]	270	3	2	2	47.2	64
Cu-Zn-Ga/SiO <sub>2</sub> [21]	270	3	2	2	99.8	128
Cu-Zn-Ga/H-SiO <sub>2</sub> [21]	270	3	2	5.6	99.5	352
Cu/ZnO/ZrO <sub>4</sub> Ga <sub>4</sub> O <sub>3</sub> [22]	250	3	8	N/A	75	324
Cu/ZnGa <sub>4</sub> O <sub>4</sub> [23]	240	2.8	4.5	26	48	N/A
Cu/SiO <sub>2</sub> [24]	250	3	4.1	2.8	15	N/A
Pd/SiO <sub>2</sub> [24]	250	3	4.1	3.0	23	N/A
Pd-Zn/CNT [25]	270	3	5	19.6	35.5	343
Pd-Ga/CNT [26]	250	3	5	16.5	52.5	512
Pd/Ga <sub>2</sub> O <sub>3</sub> [27]	250	3	5	17.3	51.6	175.6
Ga <sub>4</sub> O <sub>3</sub> -Pd/SiO <sub>4</sub> [28]	250	3	3	1.34	58.9	283.4
Pd-CaO/MCM-41 [29]	250	3	3	12.1	65.2	N/A
In <sub>2</sub> O <sub>3</sub> /ZrO <sub>2</sub> [30]	300	4	5	5.2	99.8	295
In <sub>2.5</sub> /ZrO <sub>2</sub> [31]	300	4	5	5.7	46.5	160
In <sub>2</sub> O <sub>3</sub> [32]	270	3	4	1.1	54.9	25
In <sub>2</sub> O <sub>3</sub> [32]	330	3	4	7.1	40.0	118
ZnO-ZrO <sub>2</sub> [33]	320	4	5	10	91.0	730

### 2.1. Cu-Based Catalysts

Diving into the intricacies of Cu-based catalysts, they have been the cornerstone of CO<sub>2</sub> hydrogenation for methanol synthesis for decades, primarily because of their cost-effectiveness. The industrially popular Cu-ZnO-Al<sub>2</sub>O<sub>3</sub> is a testament to the synergy between Cu and ZnO, with Al<sub>2</sub>O<sub>3</sub> playing a role in maintaining structural integrity by preventing the agglomeration of the active metal. ZnO wears multiple hats in this synergy, both as a geometric spacer between Cu nanoparticles and as an electronic promoter. This collaboration triggers various phenomena, such as the Strong Metal Support Interaction (SMSI). Studies have further hinted at the formation of a metastable ZnO<sub>x</sub> layer on Cu nanoparticles within these catalysts [34]. The role of Zn in this matrix is subtle yet vital, significantly impacting methanol production, thereby emphasizing the importance of a thorough understanding of these interactions.

To avoid the adsorption of water by hydrophilic Al<sub>2</sub>O<sub>3</sub>, it has been proposed to use compounds with weaker hydrophilicity, such as zirconium oxide (ZrO<sub>2</sub>), as supporting materials for methanol synthesis. Given its strong heat resistance and high stability in oxidizing and reducing environments, ZrO<sub>2</sub> is considered a promising catalyst carrier [35] (Figure 3). It has been found that tetragonal ZrO<sub>2</sub> (t-ZrO<sub>2</sub>) surfaces have a higher concentration of oxygen vacancies compared with monoclinic ZrO<sub>2</sub> (m-ZrO<sub>2</sub>), indicating that the structure of ZrO<sub>2</sub> affects the concentration of oxygen vacancies in the catalyst. Samson et al. discovered that, as the t-ZrO<sub>2</sub> content increased, its catalytic activity and methanol

selectivity also increased. The authors believed that the strong interaction between highly dispersed active CuO and the t-ZrO<sub>2</sub> carrier promoted the reduction of Cu<sup>2+</sup> to Cu<sup>+</sup>/Cu<sup>0</sup>, generating a significant number of strong Lewis acid sites. Infrared spectroscopy analysis also revealed that the adsorption and dissociation of water in oxygen vacancies to produce Brønsted acid sites only occur on t-ZrO<sub>2</sub>, and t-ZrO<sub>2</sub>'s Lewis acid sites are significantly higher than those on m-ZrO<sub>2</sub> [36]. In contrast, amorphous ZrO<sub>2</sub> can stabilize tiny Cu NPs, enhance the interaction between Cu and ZrO<sub>2</sub>, and improve selectivity toward methanol. Nevertheless, the crystal structural differences in the role of Cu/ZrO<sub>2</sub> catalysts remain controversial [37].

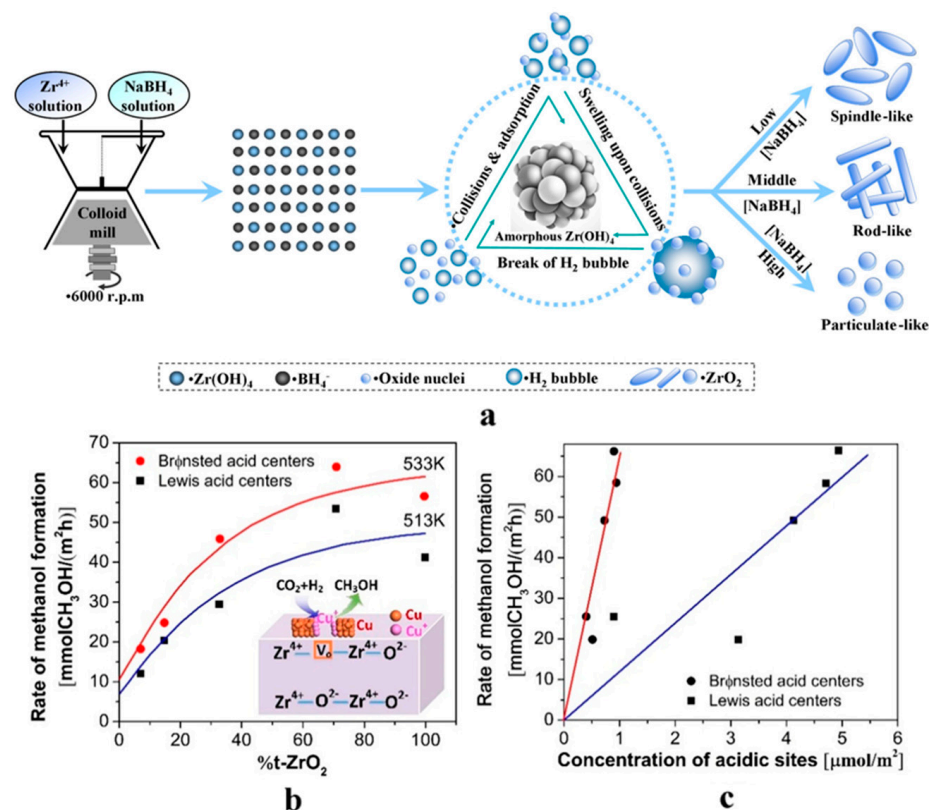


**Figure 3.** Schematic illustration of the formation mechanism of ZrO<sub>2</sub> nanostructures synthesized using different NaBH<sub>4</sub> concentrations: nucleation of the Zr(OH)<sub>4</sub> precursor, transformation of the Zr(OH)<sub>4</sub> nuclei and growth of ZrO<sub>2</sub> crystals, and formation of different ZrO<sub>2</sub> nanostructures (a). Methanol formation rate as a function of t-ZrO<sub>2</sub> content (b). Methanol formation rate at 533 K as a function of the concentration of acidic sites. (■) Lewis acid centers; (●) Brønsted acid centers (c). Reproduced from ref. [35,36] with permission from the American Chemical Society, copyright 2015 and 2014.

Compared with ZrO<sub>2</sub>, cerium oxide (CeO<sub>2</sub>) has a higher redox capability. The transformation of Ce<sup>4+</sup> into Ce<sup>3+</sup>, resulting in a significant number of oxygen defects, can significantly enhance the adsorption of oxygen-containing intermediates in oxygen vacancies. Graciani and others found that the methanol production rate of CeO<sub>x</sub>/Cu catalysts is 200 times that of Cu (111) and 14 times that of Cu/ZnO (100i). In addition, Ce<sup>4+</sup> nanoparticles coming into contact with Cu (111) promote the formation of oxygen vacancies. By introducing CeO<sub>x</sub> species to Cu (111), the adsorption and activation of CO<sub>2</sub> on the metal oxide interface are improved, establishing a new reaction pathway. The reaction mechanism indicates that, between 27 °C and 227 °C, CO<sub>2</sub> is adsorbed on the CeO<sub>2</sub> (111) surface rather than Cu (111). Compared with formate species (HCOO<sup>\*</sup>), carbonate species (CO<sub>3</sub><sup>2-</sup>) formed on the CeO<sub>2</sub> (111) surface, given their higher stability, are considered key intermediates in methanol synthesis [38]. Moreover, the morphology of the CeO<sub>2</sub> carrier also

affects the electronic structure of the active metal, enhancing the interaction between the active metal and the  $\text{CeO}_2$  carrier. Wu et al. constructed a  $\text{CeO}_2$  nanotube with a diameter of 30–50 nm. This unique nanotube structure is conducive to dispersing and reducing the Ni–Cu alloy and also promotes the adsorption and hydrogenation of intermediates. The strong interaction between the Cu–Ni alloy and  $\text{CeO}_2$  facilitates the partial reduction of  $\text{Ce}^{4+}$  into  $\text{Ce}^{3+}$ , producing a significant number of oxygen vacancies to promote the adsorption activation of  $\text{CO}_2$ , which is beneficial for the enhancement of methanol selectivity [39].

Inert silica ( $\text{SiO}_2$ ) carriers are typically inactive for methanol synthesis, and Cu/ $\text{SiO}_2$  catalysts usually favor CO formation [40]. However, when prepared with a specific method, the enhancement of the SMSI in Cu/ $\text{SiO}_2$  catalysts can also promote methanol production. Sun and his team used flame spray pyrolysis (FSP) to prepare Cu/ $\text{SiO}_2$  catalysts. The catalyst surface is rich in  $\text{Cu}^+$  sites, reaching a methanol selectivity of up to 79% when the  $\text{CO}_2$  conversion rate is 5.2% [41]. DRIFTS results also show that  $\text{Cu}^+$  species can stabilize the CO intermediate, promote the RWGS + CO hydro pathway, inhibit CO desorption, and further promote CO hydrogenation to produce  $\text{CH}_3\text{OH}$ . Additionally, titanium dioxide ( $\text{TiO}_2$ ), as an oxygen-deficient amphoteric oxide, can significantly enhance  $\text{CO}_2$  adsorption [42].  $\text{TiO}_2$  can also increase the dispersion of Cu species, providing more active sites for  $\text{CO}_2$  conversion [43]. Therefore, Cu/ $\text{TiO}_2$  catalysts have significant potential in the hydrogenation of  $\text{CO}_2$  to produce methanol.

In addition to metal oxides, other types of supports have also been investigated. Specifically, carbon nanotubes (CNTs), because of their excellent mechanical strength, thermal stability, and chemical inertness, have been extensively used as supports in the hydrogenation of  $\text{CO}_2$  to methanol [44]. Sun et al. used CNTs doped with 2.98% pyridine-nitrogen to increase the dispersion of copper (Cu) on a Cu/Zr catalyst [45]. Although the  $\text{CO}_2$  conversion rate was lower than when carbon nanofibers (CNF) were used as the carrier, the methanol selectivity reached 96%, indicating that smaller-sized Cu nanoparticles (NPs) can produce more methanol. Furthermore, the application of novel catalysts composed of metal–organic frameworks (MOFs) in the hydrogenation of  $\text{CO}_2$  to methanol has also been researched by many scientists. For instance, An et al. introduced  $\text{UiO}_{\text{bpy}}$  to Cu/ZnO catalysts, which minimized the agglomeration of Cu and the phase separation of Cu– $\text{ZnO}_x$  [46]. Because of the strong interaction between Cu NPs and MOF structures, the resulting Cu– $\text{ZnO}_x$ @MOF demonstrated a 100% selectivity to methanol (Figure 4). The reaction mechanism suggests that hydrogen dissociated on Cu can spill over into defect sites and Zr sites, while Zn and Zr species can promote the adsorption of  $\text{CO}_2$  to form bicarbonates and carbonates, which further convert to methanol.

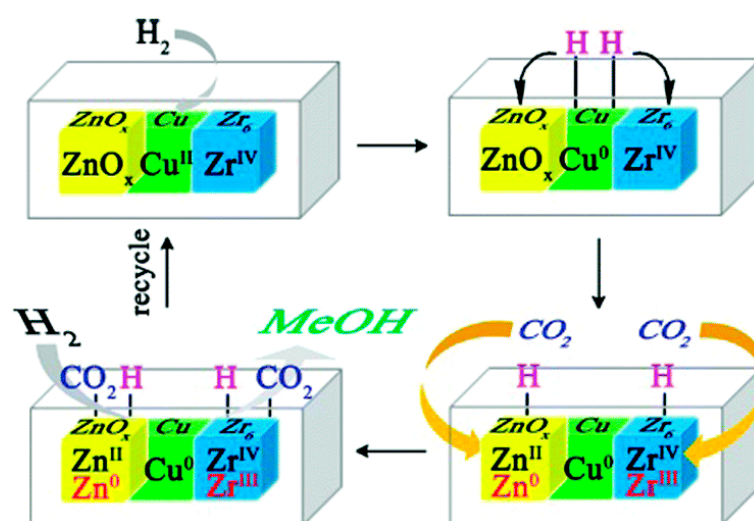


**Figure 4.** The confined active sites in MOFs and the functions of the surface sites in  $\text{CO}_2$  hydrogenation. Reproduced from ref. [46] with permission from the American Chemical Society, copyright 2017.

Incorporating promoters into Cu-based catalysts can enhance the dispersion of Cu, improve acidity–basicity and redox properties, and promote interaction and hydrogen spillover between Cu and its support [47]. Magnesium oxide (MgO), an alkaline earth metal oxide, when introduced to methanol synthesis Cu-based catalysts, can increase the catalyst surface basicity, suppressing methane formation. Additionally, the introduction of MgO promotes the reduction of CuO, leading to the formation of more Cu<sup>0</sup> species that act as the active center for CO<sub>2</sub> hydrogenation, significantly enhancing hydrogenation activity [48]. Similarly, the introduction of rare-earth metal oxides to Cu-based catalysts produces comparable effects. Ishihara and colleagues doped CeO<sub>2</sub> into Cu/Al<sub>2</sub>O<sub>3</sub> catalysts, resulting in a Cu/AlCeO catalyst that demonstrated faster methanol formation rates than a Cu/Al<sub>2</sub>O<sub>3</sub> catalyst [49]. Doping with CeO<sub>2</sub> helps suppress the growth of Cu NP sizes, promoting the formation of surface Cu<sup>+</sup> species while enhancing basic sites to improve CO<sub>2</sub> adsorption, thus lowering the reaction activation energy. Chen et al. found that introducing La species to a porous SBA-15 support can strengthen the strong interaction between Cu NPs and LaO<sub>x</sub>, leading to the formation of numerous Cu-LaO<sub>x</sub> interfaces (Figure 5). This unique interface boosts CO<sub>2</sub> adsorption, facilitating its transformation via the formate pathway, thus enhancing methanol selectivity [50]. Transition metal oxides such as ZrO<sub>2</sub> have also been employed as promoters to modify catalyst surfaces and regulate interactions between metal supports [37]. The introduction of ZrO<sub>2</sub> elevates the basicity of the catalyst surface, leading to the formation of HCO<sub>3</sub><sup>−</sup> adsorbed on the ZrO<sub>2</sub> surface. This is then further hydrogenated to form HCOO\* intermediate on the Cu surface [51]. Arena and colleagues proposed a formate pathway for the Cu-ZnO-ZrO<sub>2</sub> catalyst, suggesting that an abundance of HCOO\* intermediates promotes methanol formation [52].

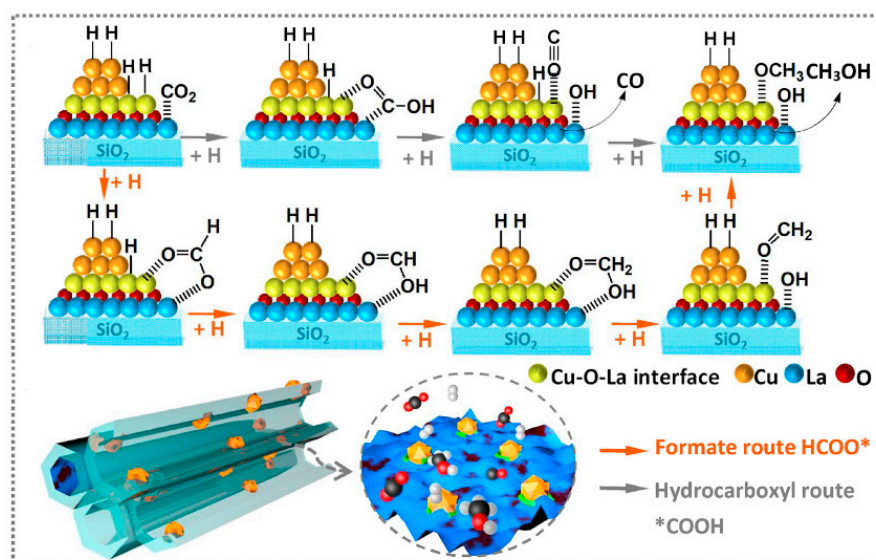


**Figure 5.** Reaction mechanism for CO<sub>2</sub> hydrogenation over Cu<sub>1</sub>La<sub>0.2</sub>/SBA-15 catalyst, through a single O atom or along the formate pathway, adsorbed through two O atoms in the bidentate configuration (\*HCOO), and further hydrogenated to the final product CH<sub>3</sub>OH. Reproduced from ref. [50] with permission from Elsevier, copyright 2019.

To develop more efficient CO<sub>2</sub> to methanol hydrogenation catalysts, precise control over the nanostructure of the catalyst becomes increasingly critical. Some specialized structures outperform conventional metal-loaded oxide catalysts. Catalysts comprising highly dispersed metal oxides on metallic nanoparticles, referred to as reverse oxide/metal catalysts, demonstrate a unique active interface with improved catalytic activity in CO<sub>2</sub> hydrogenation [53]. Ma et al. synthesized an adjustable Zr/Cu ratio reverse ZrO<sub>2</sub>/Cu catalyst through an oxalic acid co-precipitation method, revealing a methanol formation rate twice as high as the traditional Cu/ZrO<sub>2</sub> catalyst. The reverse ZrO<sub>2</sub>/Cu catalyst was

identified as partially reduced amorphous  $\text{ZrO}_2$  supported on metal Cu particles. In situ infrared results showed enhanced  $\text{CO}_2$  activation and oxygen-containing intermediate hydrogenation rates, indicating high methanol production activity [54]. Additionally, core-shell structures, consisting of active metal and a surface promoter layer, can heighten surface-adsorbed electron density and bimetallic synergistic effects [55]. An et al. found that enclosing core-shell particles within MOF support networks can further amplify the dispersion of active metals and the interaction between the metal and the support, thereby boosting catalytic activity [46].

## 2.2. Precious Metal Catalysts

While copper-based catalysts have been traditionally favored for their efficiency in  $\text{CO}_2$  hydrogenation, there has been growing interest in the application of precious metal (PM) catalysts given their unique properties and potential for enhanced catalytic performance. Recently, the potential of Au-based nano-catalysts in  $\text{CO}_2$  hydrogenation for methanol production has been recognized. Liu et al. reported that a  $\text{Au}^{\delta+}\text{-In}_2\text{O}_{3-x}$  catalyst achieved 100% methanol selectivity at 225 °C, and even at temperatures as high as 300 °C, the selectivity remained at 67.8% (Figure 6). Further studies have shown that the interface between Au nanoparticles and oxide supports plays a crucial role in promoting  $\text{CO}_2$  hydrogenation to methanol [56].

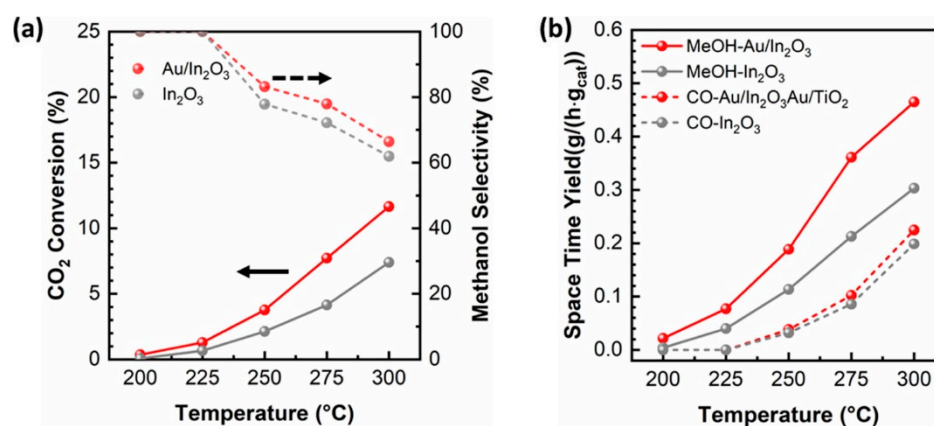


**Figure 6.** Comparison of the (a)  $\text{CO}_2$  conversion and methanol selectivity vs. temperature over  $\text{In}_2\text{O}_3$  and  $\text{Au/In}_2\text{O}_3$  catalysts; (b) STY of methanol and CO vs. temperature over  $\text{In}_2\text{O}_3$  and  $\text{Au/In}_2\text{O}_3$  catalysts. Reaction conditions: 5 MPa,  $\text{H}_2/\text{CO}_2/\text{N}_2 = 76:19:5$ , GHSV =  $21,000 \text{ cm}^3/(\text{g}_{\text{cat}} \cdot \text{h})$ . Reproduced from ref. [56] with permission from the American Chemical Society, copyright 2020.

In addition to Au, Pd-based catalysts are also widely used in methanol synthesis because of their excellent stability and sintering resistance. Notably, Pd promotes hydrogen spillover and demonstrates good adsorption and dissociation properties for hydrogen. This ensures a rich supply of hydrogen species for  $\text{CO}_2$  hydrogenation.  $\text{CeO}_2$ , known as a source of oxygen vacancies that can enhance  $\text{CO}_2$  adsorption and activation, has been selected as a carrier for Pd-based catalysts [57]. Choi et al. observed that, among Pd catalysts with a loading amount equal to 0.5–2 wt%, the one with the highest  $\text{Ce}^{3+}/\text{Ce}^{4+}$  ratio (1 wt% Pd catalyst) produced more oxygen vacancies, leading to the highest  $\text{CO}_2$  conversion and methanol yields [58]. Another study showed that a Pd/ $\text{CeO}_2$  catalyst produced a  $\text{Ce}_2\text{O}_3$  phase when reduced at 500 °C, but not at lower temperatures.  $\text{CO}_2$  adsorbed at the interface of Pd and reduced  $\text{Ce}_2\text{O}_3$  interacted with spillover hydrogen species from Pd to form CO, which subsequently hydrogenated to form methanol [59].

Metals like Pd and Pt can form alloys with metals commonly used in  $\text{CO}/\text{CO}_2$  hydrogenation, such as Pd-Cu, Pd-Zn, and Pt-Co alloys [47]. Such alloy structures can modify the chemical properties of the metal surface and offer new active sites for reactions by adjusting reduction conditions and metal components [60]. Jiang et al. co-impregnated Pd-Cu bimetal on amorphous  $\text{SiO}_2$  and found that when the atomic ratio of Pd/(Pd + Cu)

was between 0.25 and 0.34, methanol formation rates significantly surpassed that of single-metal catalysts (Figure 7). This heightened activity was attributed to the simultaneous presence of CuPd and CuPd<sub>3</sub> alloy phases in the reduced bimetallic Pd(0.34)-Cu/SiO<sub>2</sub> catalyst. These alloy phases resulted from strong synergistic effects between Cu and Pd, influenced by the Pd/(Pd + Cu) atomic ratio [24]. Furthermore, DFT studies indicated that the presence of Pd on the Cu (111) surface strengthened reactant adsorption and reduced reaction barriers, promoting the conversion of intermediate species into methanol [61]. The results showed that CO and methane formation on the PdCu (111) surface were inhibited, and a 1%Pd-promoted Cu-ZnO catalyst had a methanol yield 2.5 times higher than that of a Cu-ZnO catalyst [62].

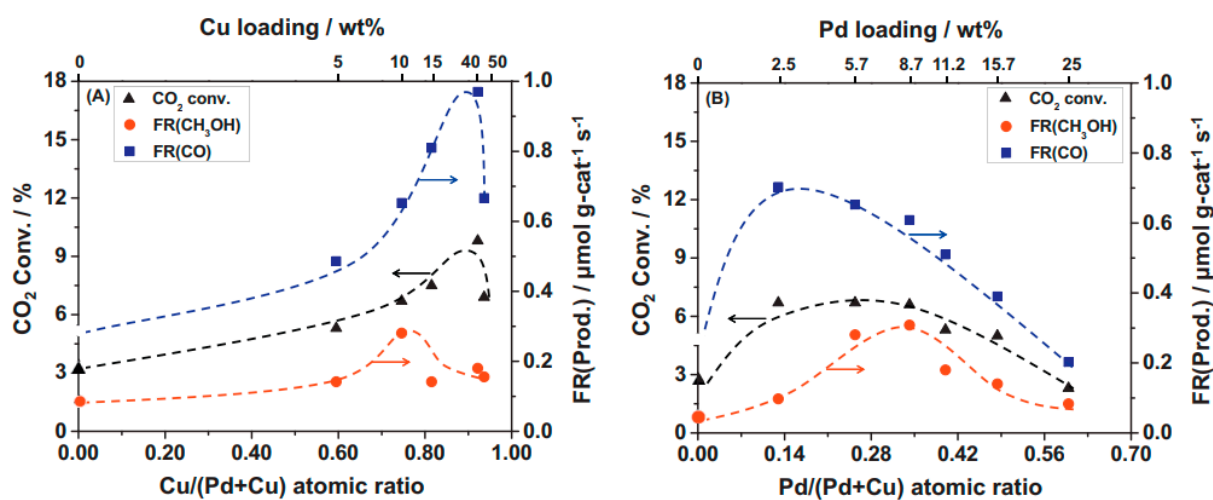


**Figure 7.** Changes in CO<sub>2</sub> conversion and formation rate of products (CH<sub>3</sub>OH and CO) over Pd–Cu(Y)/SiO<sub>2</sub> with fixed Pd loading at 5.7 wt% (A) and Pd(X)–Cu/SiO<sub>2</sub> with fixed Cu loading at 10 wt% (B) as functions of Cu/(Pd + Cu) and Pd/(Pd + Cu) atomic ratios, respectively. CO<sub>2</sub> hydrogenation: 523 K, 4.1 MPa, 6.2 g-cat h mol<sup>−1</sup>. Reproduced from ref. [24] with permission from Elsevier, copyright 2020.

### 2.3. Metal Oxide Catalysts

Recent research has illuminated the exciting potential of metal oxide catalysts in the realm of CO<sub>2</sub> hydrogenation. Notably, the surface oxygen vacancies of indium oxide (In<sub>2</sub>O<sub>3</sub>) have been identified as playing a pivotal role in achieving high selectivity and activity for methanol, thus marking In<sub>2</sub>O<sub>3</sub> as a promising catalyst for CO<sub>2</sub> hydrogenation to methanol [63] (Figure 8). Compared with non-precious metal catalysts such as Cu and Ni and even precious metal catalysts like Pt and Pd, In<sub>2</sub>O<sub>3</sub> demonstrates superior methanol selectivity. Moreover, researchers have been able to modulate the structure of In<sub>2</sub>O<sub>3</sub> and employ it as a support for other metals, thereby enhancing the adsorption and activation properties of the reactant gases [64]. Ye and his colleagues carried out DFT calculations on the adsorption configurations and hydrogenation reactions of CO<sub>2</sub> on a perfect In<sub>2</sub>O<sub>3</sub> (110) surface, providing deeper insights into the reaction mechanism [65]. Furthermore, researchers have reported different potential oxygen vacancy sites on the In<sub>2</sub>O<sub>3</sub> surface, revealing that the vacancies formed directly via thermal treatments are endothermic, while those formed in the presence of H<sub>2</sub> or CO are exothermic. The reactivity at specific sites can lead to different product outcomes [66].



**Figure 8.** The role of vacancies on the surface of an  $\text{In}_2\text{O}_3$  catalyst in  $\text{CO}_2$  hydrogenation to  $\text{CH}_3\text{OH}$ . Reproduced from ref. [66] with permission from the American Chemical Society, copyright 2013.

To harness the high methanol selectivity exhibited by  $\text{In}_2\text{O}_3$ , it has been supported on different carriers. Among these, the introduction of  $\text{ZrO}_2$  has been found to significantly enhance the intrinsic activity of the catalyst (Figure 9). Martin and collaborators revealed that an  $\text{In}_2\text{O}_3/\text{ZrO}_2$  system showcases 100% methanol selectivity and can operate continuously under industrially relevant conditions [67]. DFT results, as well as work by Zhang and colleagues [68], confirm that doping with  $\text{ZrO}_2$  can bolster  $\text{CO}_2$  adsorption and stabilize intermediate species on the Zr- $\text{In}_2\text{O}_3$  (110) surface. Moreover, Dang and his team found that oxygen defects near the Zr dopant lead to stronger  $\text{CO}_2$  adsorption than on the pure  $\text{In}_2\text{O}_3$  surface [69]. Given the high oxygen vacancy concentration in  $\text{Ga}_2\text{O}_3$ , Witoon and his group used  $\text{Ga}_x\text{In}_{2-x}\text{O}_3$  intermetallic oxides for methanol synthesis. Their findings indicate that the  $\text{Ga}_{0.4}\text{In}_{1.6}\text{O}_3$  catalyst offers the highest methanol yield.  $\text{Ni}_5\text{Ga}_3$  bimetallics were also proven to be active sites for methanol synthesis, with Sharafutdinov's research indicating that, compared with traditional  $\text{Cu}/\text{ZnO}/\text{Al}_2\text{O}_3$ , a  $\text{Ni}_5\text{Ga}_3/\text{SiO}_2$  catalyst with  $\text{Ni}_5\text{Ga}_3/\text{SiO}_2$  had the highest methanol generation [70].

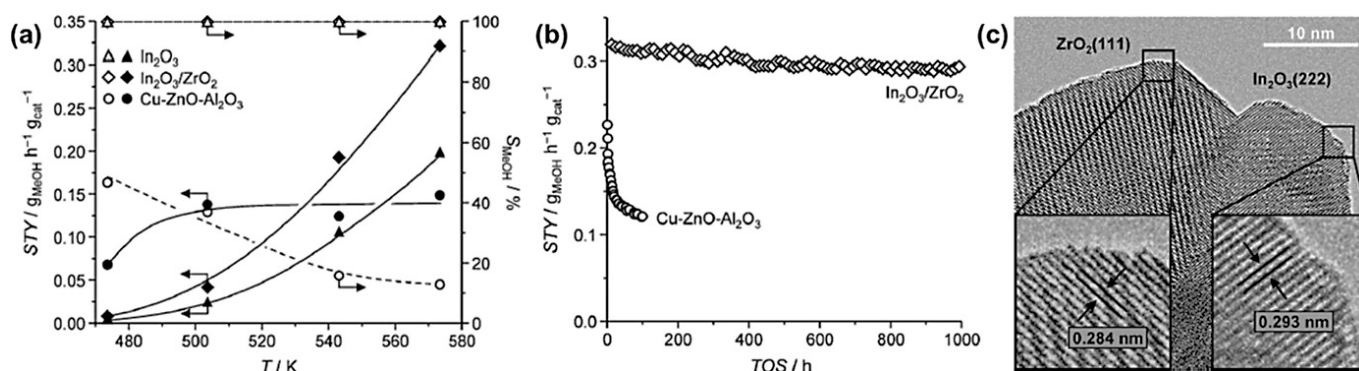


**Figure 9.** (a) Methanol STY and selectivity for  $\text{CO}_2$  hydrogenation over bulk  $\text{In}_2\text{O}_3$ ,  $\text{In}_2\text{O}_3/\text{ZrO}_2$  (9 wt%), and the benchmark  $\text{Cu-ZnO-Al}_2\text{O}_3$  catalyst at various temperatures ( $\text{CO}_2/\text{H}_2 = 1:4$ , 5.0 MPa,  $\text{GHSV} = 16,000 \text{ h}^{-1}$ ). (b) Evolution of methanol STY with time-on-stream (TOS) over  $\text{In}_2\text{O}_3/\text{ZrO}_2$  and  $\text{Cu-ZnO-Al}_2\text{O}_3$  (573 K, 5.0 MPa,  $\text{CO}_2/\text{H}_2 = 1:4$ ,  $\text{GHSV} = 16,000 \text{ h}^{-1}$ ). (c) HRTEM micrograph of the  $\text{In}_2\text{O}_3/\text{ZrO}_2$  catalyst obtained after 4 h on stream. Reproduced with permission from ref. [67]. Copyright 2016 John Wiley and Sons.

Recently, bimetallic oxide catalysts with high activity and selectivity have garnered increased attention. Wang and colleagues prepared a  $\text{ZnO-ZrO}_2$  solid solution catalyst that demonstrated high methanol selectivity and yield from  $\text{CO}_2$  hydrogenation. Given

the remarkable performance of this ZnO-ZrO<sub>2</sub> solid solution catalyst, Wang and his team further extended their research to other bimetallic oxide systems. They investigated the likes of CdZrO<sub>x</sub> and GaZrO<sub>x</sub>, looking to understand the implications of varying the metal constituents in these oxide catalysts [33]. Through their meticulous studies, they found that the synergistic interactions between the metals in these oxide combinations can notably enhance the adsorption and activation of H<sub>2</sub> and CO<sub>2</sub>. Such advancements play a pivotal role in refining the overall catalytic process.

### 3. Methanol Synthesis from CO<sub>2</sub>

The catalytic transformation of CO<sub>2</sub> into methanol is seen as a promising avenue to both address al challenges and produce valuable chemicals. Despite the strides made in this domain, there are unresolved questions that persist, particularly surrounding the exact mechanisms and active phases of the reaction. Central to the debate on CO<sub>2</sub> hydrogenation is the pathway through which methanol is produced. Some researchers propose a direct hydrogenation pathway (Figure 10). In this view, CO<sub>2</sub> undergoes a series of hydrogenation steps consecutively, beginning with the reaction of CO<sub>2</sub> with hydrogen, which produces formic acid or a related anhydride. This then undergoes further hydrogenation processes, culminating in methanol. On the other hand, there is also a strong argument for an intermediate CO pathway. Here, the initial step is the reduction of CO<sub>2</sub> into CO. This is then followed by a combination of the well-documented water–gas shift reaction and Fischer–Tropsch synthesis, eventually leading to the formation of methanol. In a third mechanism, CO<sub>2</sub> is initially activated via the H-assisted pathway to form trans-COOH. This intermediate undergoes subsequent steps of hydrogenation and isomerization, leading to the formation of COHOH\*. The latter then decomposes into COH\*, which is eventually hydrogenated to produce methanol. Nevertheless, elucidation of CO<sub>2</sub> reaction pathway is not only of interest to fundamental research but also important for industrial application. It can influence how researchers approach catalyst design, condition optimization, and even the choice of promoter elements.

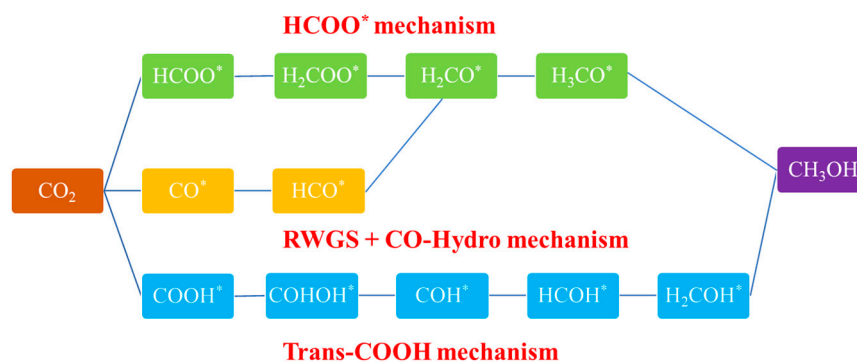


**Figure 10.** Proposed reaction mechanisms for methanol synthesis from CO<sub>2</sub> hydrogenation.

Another critical aspect of this reaction is the identification of its active phase, which is a decisive factor in catalyst development. The debate often pivots around whether the catalyst's active sites are in a metallic state or an oxidized one. Some studies lean toward metallic sites, particularly on noble metals, as being the primary drivers of catalytic activity. Yet others argue for the importance of partially or fully oxidized metal sites. Further adding to the complexity is the discussion of the nature of these active sites. Questions arise on whether single-atom active sites are primarily responsible for the reaction or if larger entities like clusters or nanoparticles are more crucial. The methodology of catalyst preparation can be significantly influenced by this knowledge, affecting decisions on nanoparticle size, interaction with supports, and the amount of metal loaded. Recent insights have also brought forth the idea that these active sites might have a dynamic nature, not remaining constant but undergoing transformations depending on the reaction conditions. This dynamism further muddies the waters in identifying the true active phase and underscores

the need for advanced characterization techniques that can track these transient species in real time.

### 3.1. Reaction Pathways of CO<sub>2</sub> Hydrogenation to Methanol

#### 3.1.1. Formate (HCOO\*) Pathway

The understanding of the formate pathway in the hydrogenation of CO<sub>2</sub> to methanol has evolved significantly thanks to a plethora of studies that have delved into the mechanistic intricacies of this reaction. The pathway is premised on a series of steps initiated by the hydrogenation of CO<sub>2</sub> to form a series of intermediates, starting with formate (HCOO\*) to methanol (Figure 11). This conversion proceeds through intermediates like dioxymethylene (H<sub>2</sub>COO\*), formaldehyde (H<sub>2</sub>CO\*), and methoxy (H<sub>3</sub>CO\*). Interestingly, research indicates that the formation of HCOO\* and H<sub>2</sub>COO\* is the rate-determining step (RDS) [71].

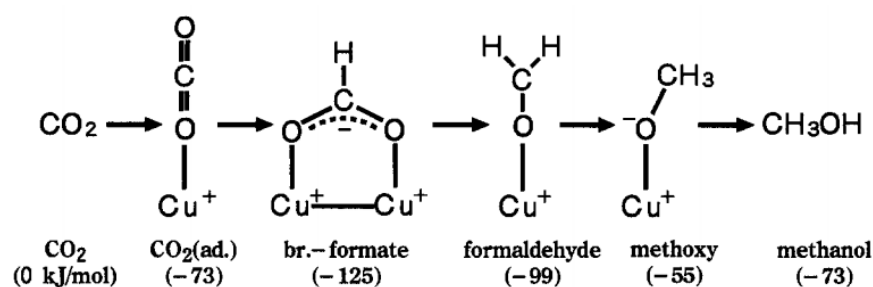


**Figure 11.** CO<sub>2</sub> hydrogenation mechanism on a Cu/ZnO catalyst. Reproduced from ref. [72] with permission from eevier, copyright 1997.

One of the foundational works in this domain, as cited, proposes a formate reaction pathway based on the Langmuir–Hinshelwood (LH) and Eley–Rideal (ER) mechanisms [73]. In a noteworthy study by Liu et al., they conducted DFT calculations on Cu (111) surfaces and unsupported Cu<sub>29</sub> NPs. Their findings showed that methanol synthesis on the Cu surface predominantly occurs via the HCOO\* intermediate. The overall reaction rate is limited by the hydrogenation of HCOO\* and H<sub>2</sub>COO\*. Notably, the Cu<sub>29</sub> NPs, because of their structural flexibility and the presence of low-coordinated Cu, can stabilize the reaction intermediates HCOO\* and H<sub>2</sub>COO\*. This stabilization makes the subsequent hydrogenation steps energetically more favorable, thus enhancing the overall catalytic activity [74].

Coperet et al. further expanded our understanding by exploring the adsorption of CO<sub>2</sub> on different surfaces. Theoretical simulations were conducted on individual Cu and ZrO<sub>2</sub> surfaces and Cu/ZrO<sub>2</sub> interface. The results of this study are particularly revealing. They found that CO<sub>2</sub> struggles to bind with the Cu (111) surface but adsorbs onto the ZrO<sub>2</sub> surface either as CO<sub>3</sub><sup>2-</sup> or HCO<sub>3</sub><sup>-</sup>. An intriguing observation was made when CO<sub>2</sub> was adsorbed at the interface of Cu and ZrO<sub>2</sub>: the carbon atom bonded with Cu, and the two oxygen atoms attached to the Zr<sub>4</sub><sup>+</sup> Lewis acidic sites on the ZrO<sub>2</sub> surface. Transition state calculations further indicated that free energy for the formation of HCOO\* is lower than for CO and carboxyl (COOH\*), thus establishing the HCOO\* pathway as the most favorable route [75]. This study emphasized the vital role of oxide supports and metal–oxide interfaces in modulating CO<sub>2</sub> activation, reaction pathways, and kinetics, eventually influencing methanol selectivity.

In a quest to comprehend the universality of the formate pathway, studies have not been limited to Cu-based catalysts. For instance, Ye et al., through DFT calculations, found that, on a pristine In<sub>2</sub>O<sub>3</sub> surface, the hydrogenation of CO<sub>2</sub> to generate the HCOO\* species is more favorable than its protonation to produce COOH\*, suggesting a selective methanol formation via the HCOO\* pathway on the In<sub>2</sub>O<sub>3</sub> (110) surface [65]. This finding was echoed by Gao et al., who identified a similar process where CO<sub>2</sub> is adsorbed at oxygen vacancies on defective oxides and progresses through the HCOO\* pathway to eventually produce

methanol. These oxygen vacancies are then regenerated in subsequent hydrogenation steps [76].

Another intriguing proposition came from Grabow et al., who combined DFT calculations with microkinetic modeling. They proposed a slightly different HCOO\* route for methanol formation on the Cu (111) surface, proceeding through  $\text{CO}_2 \rightarrow \text{HCOO} \rightarrow \text{HCOOH} \rightarrow \text{H}_2\text{COOH} \rightarrow \text{CH}_2\text{O} \rightarrow \text{CH}_3\text{O} \rightarrow \text{CH}_3\text{OH}$  [77]. This revised HCOO pathway was also supported by Nie et al. Their DFT results suggest that, compared with PdCu<sub>3</sub> (111) surfaces with higher Cu content, step-type PdCu (111) surfaces with coordinatively unsaturated Pd atoms are more favorable for CO<sub>2</sub> adsorption activation and H<sub>2</sub> dissociative hydrogenation. Throughout this reaction, the hydrogenation of HCOO\* to form HCOOH\* (the O-H bond formation step) presents the highest energy barrier, strongly influencing the rate of methanol formation [78].

### 3.1.2. RWGS + CO Hydrogenation Pathway

Beyond the HCOO\* mechanism in CO<sub>2</sub> hydrogenation to methanol, another reaction pathway exists, often referred to as the “reverse water–gas shift coupled with CO hydrogenation” or the RWGS + CO hydrogenation pathway (Figure 12). According to this mechanism, CO<sub>2</sub> undergoes hydrogenation to produce the COOH\* intermediate, which quickly dissociates into CO. Subsequently, CO is hydrogenated to generate a series of intermediates including formyl (HCO\*); formaldehyde; methoxy; and finally, methanol [7]. This RWGS + CO hydrogenation pathway is followed during the hydrogenation of CO<sub>2</sub> to methanol on various catalysts based on elements like Cu, Rh, and In [79]. For example, Yang et al., through a combination of DFT and MC simulations, explored the reaction mechanism of CO<sub>2</sub> hydrogenation on several catalysts including Cu (111), Au/Cu (111), Ni/Cu (111), Pt/Cu (111), Pd/Cu (111), and Rh/Cu (111). Among these catalysts, those doped with Pd, Rh, Ni, and Pt followed the RWGS + CO hydro route for methanol formation. Their study also revealed an interesting correlation: the binding energy of CO on these catalyst surfaces plays a pivotal role in determining methanol yields. As the binding energy of CO decreases, the methanol yield also drops [80].

Another significant study in this context was undertaken by Liu et al., who based their research on the RWGS + CO hydro pathway to understand how the surface composition of Rh-doped Cu (111) catalysts, such as Rh<sub>3</sub>Cu<sub>6</sub> (111) and Rh<sub>6</sub>Cu<sub>3</sub> (111), affects the methanol production rate. Their findings indicate that the Rh<sub>3</sub>Cu<sub>6</sub> (111) catalyst displayed a higher methanol production rate as compared with Rh<sub>6</sub>Cu<sub>3</sub> (111) [81]. Adding further depth to this discussion, Kattel and colleagues combined theoretical calculations with experiments to compare the reaction pathways of CO<sub>2</sub> on Cu/ZrO<sub>2</sub> and Cu/TiO<sub>2</sub> catalysts. Both catalysts were active for formate pathway, but methanol production on Cu/TiO<sub>2</sub> was less efficient because active sites were poisoned by the HCOO\* species. However, the synergy between Zr<sup>3+</sup> and Cu on the Cu/ZrO<sub>2</sub> catalyst facilitated the occurrence of the RWGS + CO hydro pathway and did not poison the active centers. As a result, compared with the Cu/TiO<sub>2</sub> catalyst, Cu/ZrO<sub>2</sub> exhibited superior activity and selectivity toward methanol [82].

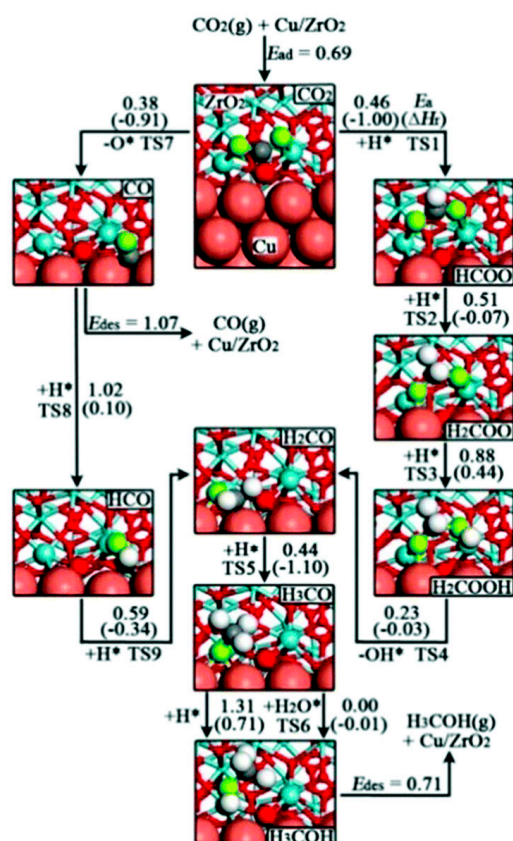


**Figure 12.** Reaction network and intermediates for methanol synthesis from CO<sub>2</sub> hydrogenation. Reproduced from ref. [83] with permission from Elsevier, copyright 2009.

### 3.1.3. Trans-COOH Pathway

Recently, the trans-COOH pathway has been proposed as an alternative route for the hydrogenation of CO<sub>2</sub> to methanol (the blue route in Figure 10). The trans-COOH pathway involves a series of steps that produce various intermediates: (1) the hydrogenation of CO<sub>2</sub> leads to the formation of a carboxyl species (COOH\*); (2) this carboxyl species undergoes further hydrogenation to form dihydroxycarbene (COHOH\*); (3) subsequent dehydroxylation results in hydroxymethylidyne (COH\*); and (4) COH\* continues to undergo hydrogenation, forming hydroxymethylene (HCOH\*) and then hydroxymethane (H<sub>2</sub>COH) [84].

An important insight from Zhao and colleagues indicates that the formation of the COH\* species is the rate-determining step in this pathway [85]. Studies have also shown that, in the presence of water produced during the reaction, the Cu (111) catalyst follows the trans-COOH pathway for the hydrogenation of CO<sub>2</sub> to methanol. Apart from copper-based catalysts, both Au/Cu-Zn-Al and Ga<sub>3</sub>Ni<sub>5</sub> (111) catalysts have been found to adhere to the trans-COOH route [86]. Diving deeper, Tang and associates employed DFT analyses on five different facets of the Ga<sub>3</sub>Ni<sub>5</sub> catalyst used for CO<sub>2</sub> hydrogenation to methanol. These facets were (001), (021), (110), (111), and (221). Of these, the Ga<sub>3</sub>Ni<sub>5</sub> (111) catalyst stood out because of its superior reactivity, which could be attributed to its lower surface energy, with the reaction proceeding via the trans-COOH pathway. In another study focusing on the Ga<sub>3</sub>Ni<sub>5</sub> (221) catalyst, the distribution of Ni and Ga species was found to favor the formation of intermediates and the adsorptive dissociation of H<sub>2</sub>. Consistently, this reaction also adhered to the trans-COOH pathway [87].

### 3.2. Insights into the Active Phase of Cu-Based CO<sub>2</sub> Hydrogenation to Methanol Catalysts

While the arena of CO<sub>2</sub> hydrogenation to methanol boasts a diverse array of catalysts, including PM catalysts and metal oxide catalysts, it is evident that Cu-based catalysts hold distinct prominence in research endeavors. The attention they receive stems not only from their promising performance but also from their potential to be scaled up and commercialized. Their unique characteristics and the ensuing debates on the nature of their active sites make them particularly intriguing. Consequently, in this section, we will pivot our discussion to delve deeper into the understanding of the active sites of Cu-based catalysts, aiming to unravel the complexities that have made them a focal point in the realm of methanol synthesis.

The development of Cu-based catalysts for the hydrogenation of CO<sub>2</sub> to methanol primarily stems from catalysts used in methanol synthesis from syngas. Even though commercial catalysts for syngas to methanol conversion, represented by certain companies, have been in use since the 1960s, the nature of the active centers, especially their state during catalysis, remains a contentious topic. It is widely believed that during the CO hydrogenation reaction, either Cu<sup>+</sup> or Cu<sup>0</sup> plays a role in adsorbing and activating CO. Hydrogen undergoes homolysis on Cu and heterolysis on ZnO, leading to the formation of the reactive species H<sup>δ+</sup> and H<sup>δ-</sup> [88].

#### 3.2.1. Chemical State of Cu Species

A prominent debate surrounds the valence state of Cu in the catalyst during the reaction, with a focus on the adsorption and activation processes between the catalyst components and reaction gases, as well as the synergistic effects between the components. Some researchers assert that metallic copper atoms are the sole active sites for methanol synthesis. Evidence from Chinchén's group suggests a strong linear relationship between methanol yield and the surface area of metallic copper [88]. Other researchers, such as Pan and Liu, have made similar observations [89,90]. Rasmussen and colleagues investigated the behavior of CO<sub>2</sub> hydrogenation on the Cu (100) surface and, upon observing only the presence of Cu<sup>0</sup>, concluded it to be the only active site [91]. Askgaard, Karelavic, Clausen, and several other researchers have also supported the role of Cu<sup>0</sup> as the active site based on various studies and characterization methods like in situ XRD [92–94].

However, there are counterarguments. Some believe that, during CO<sub>2</sub> hydrogenation, a large portion of the Cu<sup>0</sup> surface is covered by oxygenated species, suggesting that the catalyst's methanol activity might not be solely dependent on the Cu<sup>0</sup> surface area [89]. Research on Cu-based catalysts supported on various oxides has shown that, although methanol yield relates to the specific surface area of metallic copper, it is not always linear, implying the involvement of other active centers like Cu<sup>+</sup> (or Cu<sup>δ+</sup>) [95]. Early studies by Klier suggested that Cu<sup>+</sup> dissolved in ZnO was the main active site [96]. Other researchers, such as Szanyi, examined the chemical states of clean Cu (100) surfaces under methanol synthesis conditions using Auger electron spectra (Figure 13) [97]. The emergence and evolution of surface carbon and oxygen peaks are correlated with the desorption of CO and CO<sub>2</sub> species, suggesting that surface Cu species are in an oxidized state during reactions. However, other studies using techniques like DFT calculations and experimental methods have concluded that mobile Cu nanoparticles supported on ZnO are the primary active sites [98]. Arena and colleagues identified the presence of Cu<sup>+</sup> species at the metal–oxide interface in Cu/ZnO/ZrO<sub>2</sub> catalysts using infrared spectroscopy with CO as a probe molecule. Their findings suggest that the interaction between Cu and the oxide helps stabilize Cu<sup>+</sup> [99]. Jia and others detected the presence of Cu<sup>+</sup> during the reduction process, where H<sub>2</sub> adsorbed onto it [100]. Nakamura's research on copper-based catalysts supported on different carriers found a “volcano” relationship between the copper surface area, methanol activity, and surface oxygen content. They proposed that the Cu<sup>+</sup>/Cu<sup>0</sup> ratio on the surface dictates catalyst activity. This theory was further supported by other researchers who observed enhanced catalyst activity and selectivity when altering the Cu<sup>+</sup>/Cu<sup>0</sup> ratio on the catalyst surface [101].

In summary, while many researchers emphasize the significance of  $\text{Cu}^0$  as the primary active site in Cu-based catalysts for methanol synthesis, there is substantial evidence suggesting that other copper species, especially  $\text{Cu}^+$ , also play crucial roles. The exact nature and role of these active sites remain the subjects of ongoing research and debate.

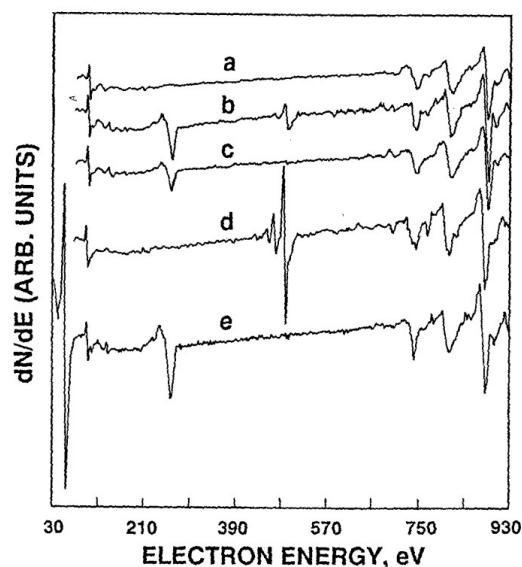


**Figure 13.** Auger electron spectra of (a) a clean Cu (100) catalyst before reaction; (b) the surface of (a) after a reaction prior to flashing to the reaction temperature under UHV conditions; (c) the surface of (b) flashed to the reaction temperature; (d) oxidized Cu (100) (2 Torr of  $\text{O}_2$ ,  $T_{\text{ox}} = 555$  K,  $t_{\text{ox}} = 5$  min); (e) the surface of (d) after reaction and a subsequent flash to 555 K. Reproduced from ref. [97] with permission from the American Chemical Society, copyright 1991.

### 3.2.2. Morphology of Metal Nanoparticles

In the  $\text{CO}_2$  hydrogenation reaction, besides the inevitable relationship between the valence state of copper and its reactivity, the morphology of copper is also vital for methanol formation. Factors such as the dispersion and morphology of metal particles determine the adsorption strength and interaction intensity between surface Cu sites and reaction intermediates [102]. The electron properties of very small grains differ from bulk metals, impacting their catalytic performance. Defects in Cu nanoparticles [103] and lattice strains [104] are considered the intrinsic active sites of the Cu surface.

Karelavic and colleagues, by adjusting the calcination temperature and copper content, prepared a series of Cu/ZnO catalysts and evaluated their  $\text{CO}_2$  hydrogenation performance. They unveiled a mechanism where catalysts with larger copper particles (10–12 nm) had higher methanol selectivity than those with smaller particles (2–3 nm), especially when the  $\text{CO}_2$  conversion rate was lower [93] (Figure 14). Some researchers believe that even if copper acts solely as an active center, clusters of metallic copper play a role, not individual copper atoms [105]. Similarly, other researchers suggest that highly dispersed metallic copper clusters are the active centers of methanol synthesis. Contrarily, findings by Natesakhawat and colleagues showed that the turnover frequency (TOF) of methanol on small-sized Cu nanoparticles was higher than on larger ones, with no correlation with the lattice strain of the Cu microcrystal, suggesting that this structural feature of copper microcrystals might not be related to their reactivity. Only  $\text{Cu}^0$  was detected on the catalyst surface both in the reduced state and after the reaction, proving the existence of the active oxidation state of copper [106]. Recent studies indicate that the active sites of industrial methanol catalysts consist of Cu “stacking faults” adorned with Zn atoms, a large number of ZnO defects, and defects in the Cu grains loaded on them [103]. However, this conclusion does not completely fit when explaining the  $\text{CO}_2$  hydrogenation reaction. Whether  $\text{Cu}^+$  is an

intermediate species during the reduction of CuO to Cu, a result of an interaction between Cu and oxide, or caused by the presence of water is still not conclusive [107].

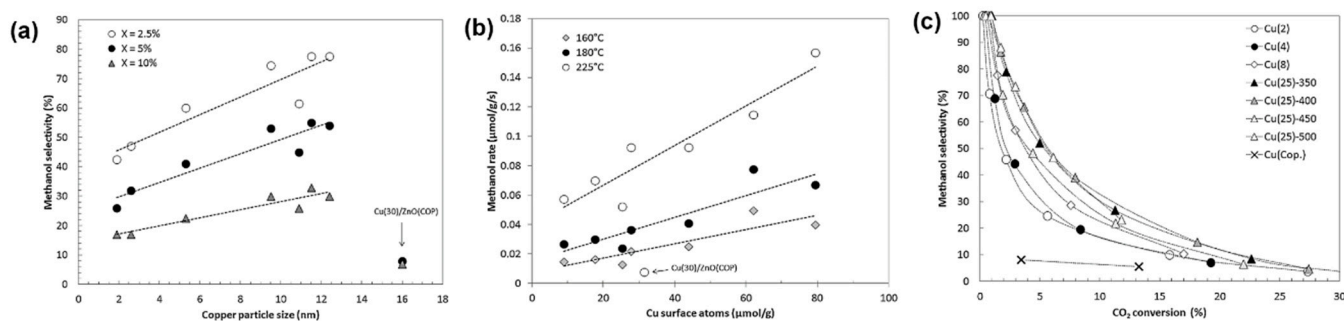


**Figure 14.** (a) Methanol selectivity as a function of copper particle size at constant conversion. Data obtained at temperatures between 140 and 250 °C. The size of copper particles was calculated using Kerkhof and Moulijn equations. (b) Forward rate of methanol formation as a function of the amount of surface copper atoms. Data for 180 and 225 °C. (c) Methanol selectivity as a function of CO<sub>2</sub> conversion. Data obtained at temperatures of 140 to 250 °C. Conditions: H<sub>2</sub>/CO<sub>2</sub> = 9 and pressure = 7 bar. Reproduced from ref. [93] with permission from Elsevier, copyright 2012.

Given the above, the conclusions on the active centers and valence state of copper during the reaction vary, and research continues in depth. Many researchers believe that the roles of Cu and oxide in catalytic reactions cannot be viewed in isolation [108]. Some think that oxides, by affecting the chemical adsorption of reactants and intermediates, control the CO<sub>2</sub> hydrogenation function of the Cu-ZnO catalytic system [109]. DFT calculations show that Cu nanoparticles loaded on the ZnO (0001) crystal face exhibit much higher CO<sub>2</sub> hydrogenation activity than the isolated Cu (111) crystal face [74]. Zhang and colleagues [110] believe that Cu<sub>2</sub>O and ZnO together form an active center, and the roles and synergies of different components in the Cu-based catalyst are drawing increasing attention.

### 3.2.3. Metal–Support Interactions

The hydrogenation of CO<sub>2</sub> to methanol utilizing Cu-based catalysts has drawn notable interest because of the intricacies and potential optimizations presented by the Strong Metal Support Interaction (SMSI). A myriad of research endeavors, employing both experimental and theoretical frameworks, has embarked on unraveling the mechanisms and characteristics of the SMSI.

A landmark observation by Fujitani et al. showed that, after a high-temperature reduction treatment of physically mixed Cu-ZnO catalysts, there is an evident ZnO<sub>x</sub> migration to the Cu particle surface (Figure 15). This observation, substantiated by TEM-EDX techniques, hints at an oxygen-covered Cu surface. Concurrently, XRD data pointed to the sporadic assimilation of ZnO into the Cu lattice, signifying the genesis of a Cu-Zn alloy [111]. The dynamism of alloy formation, as well as its subsequent decomposition under varying conditions, was captured by Topsoe using CO infrared spectroscopy absorption. This technique illuminated the continual birth and decay of the Cu-Zn surface alloy, resonating with the notion of the SMSI's temporal behavior [112]. The collaborative nature of Cu and ZnO on the catalyst surface has been at the heart of various investigative pursuits. For instance, post-roasting, an intriguing transition in the Cu/Zn ratio from 70/30 to a post-reduction state of 30/70, has been documented, a phenomenon that can be directly ascribed to SMSI effects [113].

An experiment conducted by Kurtz et al. showed that ZnO/Al<sub>2</sub>O<sub>3</sub> catalysts, under conditions mimicking industrial settings with CO/H<sub>2</sub> as the feedstock, manifested a propensity to facilitate CO hydrogenation to methanol. Elevating the operational temperature by 100 °C showcased a methanol yield mirroring what was procured from the

Cu-ZnO/Al<sub>2</sub>O<sub>3</sub> ternary catalyst. Notably, the introduction of even trace amounts of CO<sub>2</sub> to the feed could dramatically skew the activity dynamics of these catalysts [114].

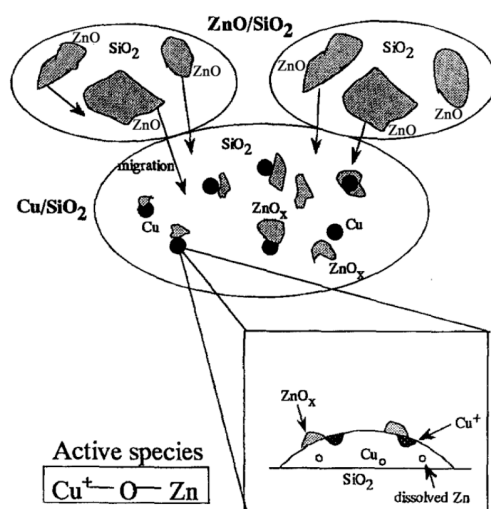


**Figure 15.** Synergy model for methanol synthesis over a physical mixture of Cu/SiO<sub>2</sub> + ZnO/SiO<sub>2</sub>. Reproduced from ref. [111] with permission from the Springer, copyright 1996.

Diving deeper, Valant's team embarked on a comprehensive exploration spanning diverse catalyst preparations. Their seminal findings showed that the Cu-ZnO synergy predominantly emerges during the reduction phase (Figure 16). The extent of this synergistic collaboration was directly proportional to the Cu-ZnO contact points, which were pivotal in spawning active oxygen vacancies [115]. Marrying experimental insights with computational prowess, Kattel and his associates leveraged density functional theory (DFT) calculations on ZnCu and Cu-ZnO model catalysts. Their hypothesis postulates that ZnCu, under the reaction milieu, undergoes oxidation, thereby forging Cu-ZnO, which then promotes its SMSI-driven collaborative action [116].

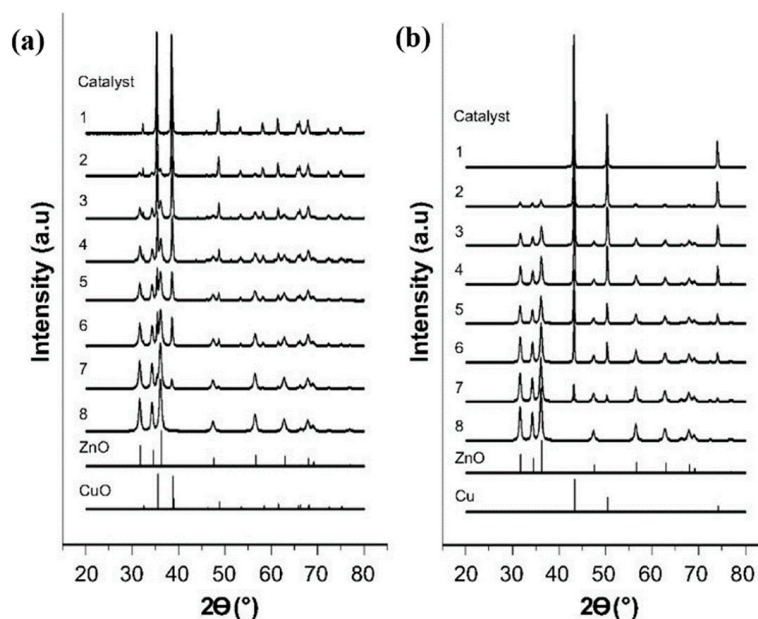


**Figure 16.** XRD patterns corresponding to (a) fresh catalysts and (b) reduced catalysts. Reproduced from ref. [115] with permission from Elsevier, copyright 2015.

In conclusion, the structure-sensitive nature of CO<sub>2</sub>'s catalytic hydrogenation to methanol highlights the cardinal role played by SMSI. The effect of SMSI can never be ignored when attempting to understand the adsorption behavior, intermediate formation, reaction pathways, as well as the structure-activity/ structure-selectivity correlations. The symbiotic dance between Cu and its oxide partners, under the aegis of SMSI, promises to chart new territories in catalyst design and efficiency for methanol synthesis.

#### 3.2.4. Active Sites of CO<sub>2</sub> Activation

CO<sub>2</sub>, the terminal oxidation state of carbon, is characterized by its linear, symmetrical, triatomic molecular structure. This inherent stability, combined with its role as a weak electron donor and a strong electron acceptor, renders its activation challenging. Successfully introducing electrons to CO<sub>2</sub> is instrumental in the activation of this inert gas molecule. Chemical adsorption activation has emerged as the most prevalent method, marking a critical step toward the industrial application of CO<sub>2</sub>. Contrasting with the extensive body of research focused on CO adsorption on metal or oxide surfaces, the domain of CO<sub>2</sub> chemical adsorption is relatively nascent. Nevertheless, as research intensifies on the hydrogenation of CO<sub>2</sub> to methanol over copper-based catalysts, CO<sub>2</sub>'s adsorption and activation on copper and oxides have garnered significant attention.

Habraken, utilizing methods like Auger electron spectroscopy (AES), low-energy electron diffraction (LEED), and ellipsometry, concluded that CO<sub>2</sub> exhibited no interaction with the Cu (111) single crystal [117]. This finding echoed Nortan's assertion that, on a copper surface, CO<sub>2</sub> predominantly exists in a physisorbed state [118]. In tandem, Chinchén et al. detected weak adsorption sites for CO<sub>2</sub> on polycrystalline copper using gas adsorption spectroscopy [119]. Wachs and colleagues found that 99% of CO<sub>2</sub> adsorbed on the Cu (110) single crystal at −93 °C subsequently decomposed into CO and surface oxygen species [120]. Drawing on these findings, Hadden et al., leveraging the <sup>14</sup>C tracer technique, studied the adsorption and dissociation behavior of CO<sub>2</sub> on copper powder surfaces reduced at 240 °C. Their observations indicated that the chemical adsorption of CO<sub>2</sub> increased over time. Initially, CO<sub>2</sub> was weakly adsorbed onto the pristine copper surface, serving as an activated precursor. This precursor then transitioned into adsorbed CO and surface oxygen species. The oxidized copper surface exhibited an enhanced affinity for CO<sub>2</sub>, subsequently undergoing hydrogenation to form formate, culminating in methanol production [121].

In subsequent research, Sakakini et al. pinpointed the active sites of CO<sub>2</sub> on the Cu (110) and Cu (211) facets in H<sub>2</sub>-reduced Cu/ZnO/Al<sub>2</sub>O<sub>3</sub> catalysts. Notably, upon re-reducing the CO<sub>2</sub>-oxidized copper surface with H<sub>2</sub>, its initial state was restored. As photoelectron spectroscopy technologies have advanced, in-depth insights have been gleaned into CO<sub>2</sub> adsorption on copper surfaces [122]. Copperthwaite documented the adsorption of multilayer CO<sub>2</sub> on clean copper surfaces at −193 °C. During the heating process, CO<sub>2</sub> species formed and dissociated into CO and O between −183 °C and −143 °C. Furthermore, anionic CO<sub>2</sub><sup>−</sup> became more stabilized through solvation effects with neighboring CO<sub>2</sub> [123]. Rodríguez proposed that the interfaces between metals and metal carbides serve as activation sites for CO<sub>2</sub> [124]. Another line of thought suggests that the presence of Cu<sup>+</sup> enhances CO<sub>2</sub> adsorption, promoting its transformation into intermediates that further produce methanol [125].

Collectively, these studies hint at the ostensibly weak adsorption of CO<sub>2</sub> on copper surfaces. Upon delving deeper, it emerges that only specific facets exhibit an adsorption effect. In copper/oxide catalysts, oxides have a more pronounced effect on CO<sub>2</sub> adsorption and activation. Given the hydroxyl and oxygen species on metal oxide surfaces, the adsorption process of CO<sub>2</sub> on these surfaces is intrinsically complex.

Aurox et al. embarked on a meticulous investigation, determining the adsorption heat of CO<sub>2</sub> on 18 different metal oxides using microcalorimetry (Figure 17). By juxtaposing their findings with infrared spectra, they identified a myriad of adsorbed surface species on metal oxides, including monodentate carbonates, bidentate carbonates, surface CO<sub>2</sub>,

and bicarbonates. The diversity in adsorbed species, coupled with variations in adsorption strength, led to vast disparities in adsorption heat and strength for metal oxides [126]. Building on this, Bianchi et al. explored the adsorption modes of CO<sub>2</sub> on ZrO<sub>2</sub>. With temperature-programmed desorption (TPD) and infrared results in hand, a part of CO<sub>2</sub> adsorption on ZrO<sub>2</sub> was found to be reversible. A desorption peak at 350 °C typified the bidentate bicarbonate species. After treating ZrO<sub>2</sub> at 700 °C to remove hydroxyl groups, a sharp reduction in the corresponding absorption peak was discerned from CO<sub>2</sub>-TPD infrared spectra [127].

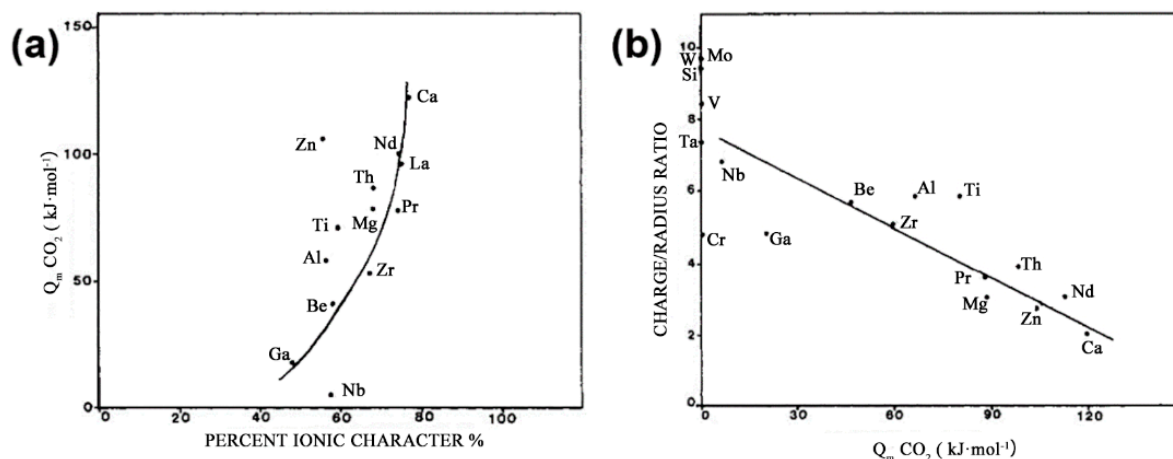


**Figure 17.** Average heats of CO<sub>2</sub> adsorption as a function of percentage of ionic character. (a) Charge/radius ratio as a function of the average heat of CO<sub>2</sub> adsorption (b). Reproduced from ref. [126] with permission from the American Chemical Society, copyright 1990.

#### 4. Conclusions and Perspective

In summary, the pursuit of ways to transform CO<sub>2</sub> into methanol is underpinned by advances in both the choice of materials and an understanding of the underlying mechanisms. Copper-based catalysts, notably Cu/ZnO/Al<sub>2</sub>O<sub>3</sub>, have consistently emerged as frontrunners in this conversion. A lively debate surrounds the exact reaction mechanism and the true nature of the active sites on these copper-based catalysts. While some researchers posit that CO<sub>2</sub> directly hydrogenates to methanol, others suggest the necessity of CO as an intermediate. Central to this discussion is the activation of CO<sub>2</sub>. Given its inherent stability and linear symmetry, the activation of this molecule is a critical step, and studies have proposed different pathways, with varying degrees of adsorption and subsequent reactions. This debate, in large part, stems from differing experimental setups, varied methodologies in characterization, and the presence of confounding factors, such as the hydrogen spillover effects. This phenomenon, wherein adsorbed active species transfer from a primary site to a secondary one, complicates our understanding of the reaction's true locus and sequence, leading to different interpretations of results across studies. Furthermore, the intricate balance of conditions—temperature, pressure, and the presence of certain elements like cerium and gallium—also influences outcomes, adding more layers to the debate. These conditions do not just affect conversion efficiency but also the very nature of the sites on the catalyst, possibly altering the active sites and thus the perceived mechanism.

At present, copper-based (Cu-based) catalysts dominate this domain, owing to their excellent catalytic prowess coupled with cost-efficiency. However, as selectivity edges beyond 80%, the methanol production rate sees a significant dip. An inevitable byproduct, water, surfaces during the reaction, adversely affecting the longevity of Cu-based catalysts. Innovations such as the development of membrane reactors present a solution, effectively separating the produced water, and thereby enhancing catalyst stability.

While noble metals offer catalytic promise, their exorbitant costs limit their widespread application in CO<sub>2</sub> hydrogenation to methanol. Emerging from this conundrum are single-atom alloys, comprising non-noble metals (like Cu) in conjunction with noble metal atoms. These are earmarked as prospective game changers in catalysis. Additionally, single-atom catalysts and supported metal cluster compounds have already demonstrated exemplary catalytic performance in pivotal reactions, underscoring their significant potential. In the realm of supported catalysts, the nature of the carrier is pivotal, playing a defining role in establishing metal–carrier interfaces, thereby determining catalyst activity and product selectivity. Factors such as acid–base sites on the catalyst surface profoundly influence CO<sub>2</sub> adsorption and activation. Simultaneously, the carrier’s structure, particularly its porous architecture, can stabilize metal nanoparticles, bolstering the mass transfer of H<sub>2</sub> and CO<sub>2</sub>. Furthermore, the efficacy showcased by inverse catalysts in CO<sub>2</sub> transformations paves the way for further explorations of innovative catalyst structures and novel preparation techniques, like wet chemical methods and oxidation methods.

In contrast to methanol synthesis, CO<sub>2</sub> hydrogenation to ethanol poses greater challenges. In the current catalyst landscape, while Rh-based and other noble metal catalysts have made their mark, modified non-noble metal catalysts, notably Cu and Co, hold the advantage in cost-effectiveness. However, a recurring issue with these catalysts is their lackluster ethanol selectivity. Addressing these concerns, research avenues focus on strategically designing efficient ethanol synthesis catalysts. One approach delves into the development of new dual-functional active sites, catering to both carbon chain elongation and alcohol formation, vital aspects of ethanol synthesis. Recent breakthroughs have spotlighted Cu-based, Pd-based, and In<sub>2</sub>O<sub>3</sub> catalysts for methanol production, alongside high-activity Fe-based and Co-based catalysts for long-chain hydrocarbon synthesis. Merging these catalyst functionalities presents a promising route to discovering new ethanol synthesis catalyst systems. Another avenue explores the atomic-scale adjustment of active sites. Recent findings highlight that tweaking the distance between Cu–Cu sites in the catalyst can bolster ethanol synthesis. Consequently, fine-tuning such dual sites at the atomic level can foster synergistic interactions between alcohol synthesis and carbon chain growth, further amplifying ethanol production.

In conclusion, as the field continues to evolve, these new insights and directions not only promise enhanced CO<sub>2</sub> to methanol and ethanol conversions but also pave the way for more sustainable and efficient pathways in green chemistry.

**Author Contributions:** Conceptualization, Z.-W.L. and Y.-F.H.; Writing—original draft preparation, M.Z. and Z.Y.; Writing—review and editing, D.G., J.W. and S.D.; Supervision, Z.-W.L.; Project administration, Z.-W.L.; Funding acquisition, Z.Y., M.Z., Y.-F.H. and Z.-W.L. All authors have read and agreed to the published version of the manuscript.

**Funding:** This research received no external funding or This research was funded by the National Key R&D Program of China (2022YFB3805504), the National Natural Science Funds of China (22378118, 22078089, 2223000258, 22238003), the Shanghai Special Program for Fundamental Research (22TQ1400100-7), the Basic Research Program of Science and Technology Commission of Shanghai Municipality (22JC1400600), SINOPEC (No. 421056), and the Open Fund of the State Key Laboratory of Chemical Engineering (GZA01220102).

**Data Availability Statement:** Data sharing not applicable.

**Conflicts of Interest:** The authors declare no conflict of interest.

## References

1. Xue, B.L.Y.; Wang, C. Progress on carbon capture, storage and utilization technology and coal seam CO<sub>2</sub> storage. *Chem. World* **2020**, *61*, 294–297.
2. Jiang, K.; Ashworth, P.; Zhang, S.; Liang, X.; Sun, Y.; Angus, D. China’s carbon capture, utilization and storage (CCUS) policy: A critical review. *Renew. Sustain. Energy Rev.* **2020**, *119*, 109601. [[CrossRef](#)]
3. Li, Q.W.Z.; Lou, S. Research progress in methanol production from carbon dioxide hydrogenation. *Mod. Chem. Ind.* **2019**, *39*, 19–23.

4. McFarlan, A. Techno-economic assessment of pathways for electricity generation in northern remote communities in Canada using methanol and dimethyl ether to replace diesel. *Renew. Sustain. Energy Rev.* **2018**, *90*, 863–876. [[CrossRef](#)]
5. Goepfert, A.; Czaun, M.; Jones, J.P.; Prakash, G.K.S.; Olah, G.A. recycling of carbon dioxide to methanol and derived products—Closing the loop. *Chem. Soc. Rev.* **2014**, *43*, 7995–8048. [[CrossRef](#)]
6. Olah, G.A.; Prakash, G.K.S.; Goepfert, A. Anthropogenic Chemical Carbon Cycle for a Sustainable Future. *J. Am. Chem. Soc.* **2011**, *133*, 12881–12898. [[CrossRef](#)]
7. Zhong, J.; Yang, X.; Liang, Z.; Huang, B.; Zhang, Y. State of the art and perspectives in heterogeneous catalysis of CO<sub>2</sub> hydrogenation to methanol. *Chem. Soc. Rev.* **2020**, *49*, 1385–1413. [[CrossRef](#)]
8. Shen, W.J.; Jun, K.W.; Choi, H.S.; Lee, K.W. Thermodynamic investigation of methanol and dimethyl ether synthesis from CO<sub>2</sub> hydrogenation. *Korean J. Chem. Eng.* **2000**, *17*, 210–216. [[CrossRef](#)]
9. Ipatieff, V.N.; Monroe, G.S. Synthesis of methanol from carbon dioxide and hydrogen over Copper-Alumina catalysts. mechanism of reaction. *J. Am. Chem. Soc.* **2002**, *67*, 2168–2171. [[CrossRef](#)]
10. Zhang, Z.L.F.; Kebin, C. New development of methanol technology. *Liaoning Chem. Ind.* **2001**, *30*, 4.
11. Ling, Y.; Luo, J.; Ran, Y.; Liu, Z.; Li, W.-X.; Yang, F. Atomic-Scale Visualization of Heterolytic H<sub>2</sub> Dissociation and CO<sub>x</sub> Hydrogenation on ZnO under Ambient Conditions. *J. Am. Chem. Soc.* **2023**, *145*, 22697–22707. [[CrossRef](#)] [[PubMed](#)]
12. Wang, Y.; Lin, S.; Li, M.; Zhu, C.; Yang, H.; Dong, P.; Lu, M.; Wang, W.; Cao, J.; Liu, Q.; et al. Boosting CO<sub>2</sub> hydrogenation of Fe-based monolithic catalysts via 3D printing technology-induced heat/mass-transfer enhancements. *Appl. Catal. B Environ.* **2024**, *340*, 123211. [[CrossRef](#)]
13. Liu, Y.; Li, Z.; Luo, P.; Cui, N.; Wang, K.; Huang, W. Size-dependent and sensitivity of copper particle in ternary CuZnAl catalyst for syngas to ethanol. *Appl. Catal. B Environ.* **2023**, *336*, 122949. [[CrossRef](#)]
14. Wei, Z.Z.; Bai, B.; Bai, H.; Duan, Y.L.; Yang, M.X.; Cao, H.J.; Zuo, Z.J.; Zuo, J.P.; Wang, Q.; Huang, W. Mechanistic exploration of syngas conversion at the interface of graphene/Cu(111): Identifying the effect of promoted electron transfer on the product selectivity. *Catal. Sci. Technol.* **2023**. [[CrossRef](#)]
15. Luk, H.T.; Novak, G.; Safonova, O.V.; Siol, S.; Stewart, J.A.; Curulla Ferré, D.; Mondelli, C.; Pérez-Ramírez, J. CO<sub>2</sub>-Promoted Catalytic Process Forming Higher Alcohols with Tunable Nature at Record Productivity. *ChemCatChem* **2020**, *12*, 2732–2744. [[CrossRef](#)]
16. Kunkes, E.L.; Studt, F.; Abild-Pedersen, F.; Schlögl, R.; Behrens, M. Hydrogenation of CO<sub>2</sub> to methanol and CO on Cu/ZnO/Al<sub>2</sub>O<sub>3</sub>: Is there a common intermediate or not? *J. Catal.* **2015**, *328*, 43–48. [[CrossRef](#)]
17. Zhu, J.; Su, Y.; Chai, J.; Muravev, V.; Hensen, E.J.M. Mechanism and Nature of Active Sites for Methanol Synthesis from CO/CO<sub>2</sub> on Cu/CeO<sub>2</sub>. *ACS Catal.* **2020**, *10*, 11532–11544. [[CrossRef](#)]
18. Nielsen, N.D.; Jensen, A.D.; Christensen, J.M. The roles of CO and CO<sub>2</sub> in high pressure methanol synthesis over Cu-based catalysts. *J. Catal.* **2021**, *393*, 324–334. [[CrossRef](#)]
19. Bansode, A.; Tidona, B.; Rohr, P.R.V.; Urakawa, A. Impact of K and Ba promoters on CO<sub>2</sub> hydrogenation over Cu/Al<sub>2</sub>O<sub>3</sub> catalysts at high pressure. *Catal. Sci. Technol.* **2013**, *3*, 767–778. [[CrossRef](#)]
20. Ladera, R.; Pérez-Alonso, F.J.; González-Carballo, J.M.; Ojeda, M.; Rojas, S.; Fierro, J.L.G. Catalytic valorization of CO<sub>2</sub> via methanol synthesis with Ga-promoted Cu–ZnO–ZrO<sub>2</sub> catalysts. *Appl. Catal. B Environ.* **2013**, *142*, 241–248. [[CrossRef](#)]
21. Toyir, J.; Piscina, P.R.R.D.L.; Fierro, J.L.G.; Homs, N.S. Highly effective conversion of CO<sub>2</sub> to methanol over supported and promoted copper-based catalysts: Influence of support and promoter. *Appl. Catal. B Environ.* **2001**, *29*, 207–215. [[CrossRef](#)]
22. Słoczyński, J.; Grabowski, R.; Olszewski, P.; Kozłowska, A.; Stoch, J.; Lachowska, M.; Skrzypek, J. Effect of metal oxide additives on the activity and stability of Cu/ZnO/ZrO<sub>2</sub> catalysts in the synthesis of methanol from CO<sub>2</sub> and H<sub>2</sub>. *Appl. Catal. A Gen.* **2006**, *310*, 127–137. [[CrossRef](#)]
23. Li, M.J.; Zeng, Z.; Liao, F.; Hong, X.; Tsang, S.C.E. Enhanced CO<sub>2</sub> hydrogenation to methanol over CuZn nanoalloy in Ga modified Cu/ZnO catalysts. *J. Catal.* **2016**, *343*, 157–167. [[CrossRef](#)]
24. Jiang, X.; Koizumi, N.; Guo, X.; Song, C. Bimetallic Pd-Cu Catalysts for Selective CO<sub>2</sub> Hydrogenation to Methanol. *Appl. Catal. B Environ.* **2015**, *170–171*, 173–185. [[CrossRef](#)]
25. Liang, X.L.; Xie, J.R.; Liu, Z.M. A Novel Pd-decorated Carbon Nanotubes-promoted Pd-ZnO Catalyst for CO<sub>2</sub> Hydrogenation to Methanol. *Catal. Lett.* **2015**, *145*, 1138–1147. [[CrossRef](#)]
26. Kong, H.; Li, H.Y.; Zhang, L.H.B. Pd-Decorated CNT-Promoted Pd-Ga<sub>2</sub>O<sub>3</sub> Catalyst for Hydrogenation of CO<sub>2</sub> to Methanol. *Catal. Lett.* **2011**, *141*, 886–894. [[CrossRef](#)]
27. Qu, J.; Xu, F.; Zhou, X. Shape Effect of Pd-Promoted Ga<sub>2</sub>O<sub>3</sub> Nanocatalysts for Methanol Synthesis by CO<sub>2</sub> Hydrogenation. *J. Phys. Chem. C. Nanomater. Interfaces* **2014**, *118*, 24452–24466. [[CrossRef](#)]
28. Collins, S.E.; Chiavassa, D.L.; Bonivardi, A.L.; Baltanás, M.A. Hydrogen Spillover in Ga<sub>2</sub>O<sub>3</sub>–Pd/SiO<sub>2</sub> Catalysts for Methanol Synthesis from CO<sub>2</sub>/H<sub>2</sub>. *Catal. Lett.* **2005**, *103*, 83–88. [[CrossRef](#)]
29. Song, Y.; Liu, X.; Xiao, L.; Wu, W.; Zhang, J. Pd-Promoter/MCM-41: A Highly Effective Bifunctional Catalyst for Conversion of Carbon Dioxide. *Catal. Lett.* **2015**, *145*, 1272–1280. [[CrossRef](#)]
30. Martin, O.; Martín, D.A.J.; Mondelli, C.; Mitchell, S.; Segawa, T.F.; Hauert, R.; Drouilly, C.; Curulla-Ferré, D.D.; Pérez-Ramírez, P.J. Indium Oxide as a Superior Catalyst for Methanol Synthesis by CO<sub>2</sub> Hydrogenation. *Angew. Chem. Int. Ed.* **2016**, *55*, 6261–6265. [[CrossRef](#)]

31. Chen, T.-Y.; Chen, C.; Ding, T.-B.; Huang, X.; Shen, H.; Cao, L.; Zhu, X.; Xu, M.; Gao, J.; Han, J.; et al. Unraveling Highly Tunable Selectivity in CO<sub>2</sub> Hydrogenation over Bimetallic In-Zr Oxide Catalysts. *ACS Catal.* **2019**, *9*, 8785–8797. [[CrossRef](#)]
32. Sun, K.; Fan, Z.; Ye, J.; Yan, J.; Ge, Q.; Li, Y.; He, W.; Yang, W.; Liu, C. Hydrogenation of CO<sub>2</sub> to methanol over In<sub>2</sub>O<sub>3</sub> catalyst. *J. CO<sub>2</sub> Util.* **2015**, *12*, 1–6. [[CrossRef](#)]
33. Wang, J.; Li, G.; Li, Z.; Tang, C.; Feng, Z.; An, H.; Liu, H.; Liu, T.; Li, C. A highly selective and stable ZnO-ZrO<sub>2</sub> solid solution catalyst for CO<sub>2</sub> hydrogenation to methanol. *Sci. Adv.* **2017**, *3*, e1701290. [[CrossRef](#)] [[PubMed](#)]
34. Lunkenbein, T.; Schumann, J.; Behrens, M.; Schloegl, R.; Willinger, M.G. Formation of a ZnO Overlayer in Industrial Cu/ZnO/Al<sub>2</sub>O<sub>3</sub> Catalysts Induced by Strong Metal-Support Interactions. *Angew. Chem.-Int. Ed.* **2015**, *54*, 4544–4548. [[CrossRef](#)]
35. Cao, W.; Kang, J.; Fan, G.; Yang, L.; Li, F. Fabrication of Porous ZrO<sub>2</sub> Nanostructures with Controlled Crystalline Phases and Structures via a Facile and Cost-Effective Hydrothermal Approach. *Ind. Eng. Chem. Res.* **2015**, *54*, 12795–12804. [[CrossRef](#)]
36. Samson, K.; Sliwa, M.; Socha, R.P. Influence of ZrO<sub>2</sub> Structure and Copper Electronic State on Activity of Cu/ZrO<sub>2</sub> Catalysts in Methanol Synthesis from CO<sub>2</sub>. *ACS Catal.* **2014**, *4*, 3730–3741. [[CrossRef](#)]
37. Li, K.; Chen, J.G. CO<sub>2</sub> Hydrogenation to Methanol over ZrO<sub>2</sub>-Containing Catalysts: Insights into ZrO<sub>2</sub> Induced Synergy. *ACS Catal.* **2019**, *9*, 7840–7861. [[CrossRef](#)]
38. Graciani, J.; Mudiyansele, K.; Xu, F.; Baber, A.E.; Evans, J.; Senanayake, S.D.; Stacchiola, D.J.; Liu, P.; Hrbek, J.; Sanz, J.F.; et al. Highly active copper-ceria and copper-ceria-titania catalysts for methanol synthesis from CO<sub>2</sub>. *Science* **2014**, *345*, 546–550. [[CrossRef](#)]
39. Tan, Q.; Shi, Z.; Wu, D. CO<sub>2</sub> Hydrogenation to Methanol over a Highly Active Cu-Ni/CeO<sub>2</sub>-Nanotube Catalyst. *Ind. Eng. Chem. Res.* **2018**, *57*, 10148–10158. [[CrossRef](#)]
40. Yang, H.; Gao, P.; Zhang, C.; Zhong, L.; Li, X.; Wang, S.; Wang, H.; Wei, W.; Sun, Y. Core-shell structured Cu@m-SiO<sub>2</sub> and Cu/ZnO@m-SiO<sub>2</sub> catalysts for methanol synthesis from CO<sub>2</sub> hydrogenation. *Catal. Commun.* **2016**, *84*, 56–60. [[CrossRef](#)]
41. Yu, J.; Yang, M.; Zhang, J.; Ge, Q.; Zimina, A.; Pruessmann, T.; Zheng, L.; Grunwaldt, J.-D.; Sun, J. Stabilizing Cu<sup>+</sup> in Cu/SiO<sub>2</sub> Catalysts with a Shattuckite-Like Structure Boosts CO<sub>2</sub> Hydrogenation into Methanol. *ACS Catal.* **2020**, *10*, 14694–14706. [[CrossRef](#)]
42. Liu, C.; Guo, X.; Guo, Q.; Mao, D.; Yu, J.; Lu, G. Methanol synthesis from CO<sub>2</sub> hydrogenation over copper catalysts supported on MgO-modified TiO<sub>2</sub>. *J. Mol. Catal. A Chem.* **2016**, *425*, 86–93. [[CrossRef](#)]
43. Chang, K.; Wang, T.; Chen, J.G. Hydrogenation of CO<sub>2</sub> to methanol over CuCeTiOx catalysts. *Appl. Catal. B Environ. Int. J. Devoted Catal. Sci. Its Appl.* **2017**, *206*, 704–711. [[CrossRef](#)]
44. Wang, G.; Chen, L.; Sun, Y.; Wu, J.; Fu, M.; Ye, D. Carbon dioxide hydrogenation to methanol over Cu/ZrO<sub>2</sub>/CNTs: Effect of carbon surface chemistry. *RSC Adv.* **2015**, *5*, 45320–45330. [[CrossRef](#)]
45. Sun, Y.; Chen, L.; Bao, Y.; Wang, G.; Zhang, Y.; Fu, M.; Wu, J.; Ye, D. Roles of nitrogen species on nitrogen-doped CNTs supported Cu-ZrO<sub>2</sub> system for carbon dioxide hydrogenation to methanol. *Catal. Today* **2018**, *307*, 212–223. [[CrossRef](#)]
46. An, B.; Zhang, J.; Cheng, K.; Ji, P.; Wang, C.; Lin, W. Confinement of Ultrasmall Cu/ZnO<sub>x</sub> Nanoparticles in Metal-Organic Frameworks for Selective Methanol Synthesis from Catalytic Hydrogenation of CO<sub>2</sub>. *J. Am. Chem. Soc.* **2017**, *139*, 3834. [[CrossRef](#)]
47. Jiang, X.; Nie, X.; Guo, X.; Song, C.; Chen, J.G. Recent Advances in Carbon Dioxide Hydrogenation to Methanol via Heterogeneous Catalysis. *Chem. Rev.* **2020**, *120*, 7984–8034. [[CrossRef](#)]
48. Ren, H.; Xu, C.H.; Zhao, H.Y.; Wang, Y.X.; Liu, J.; Liu, J.Y. Methanol synthesis from CO<sub>2</sub> hydrogenation over Cu/γ-Al<sub>2</sub>O<sub>3</sub> catalysts modified by ZnO, ZrO<sub>2</sub> and MgO. *J. Ind. Eng. Chem.* **2015**, *28*, 261–267. [[CrossRef](#)]
49. Li, S.; Guo, L.; Ishihara, T. Hydrogenation of CO<sub>2</sub> to methanol over Cu/AlCeO catalyst. *Catal. Today* **2019**, *339*, 352–361. [[CrossRef](#)]
50. Chen, K.; Fang, H.; Wu, S.; Liu, X.; Zheng, J.; Zhou, S.; Duan, X.; Zhuang, Y.; Tsang, S.C.E.; Yuan, Y. CO<sub>2</sub> hydrogenation to methanol over Cu catalysts supported on La-modified SBA-15: The crucial role of Cu-LaOx interfaces. *Appl. Catal. B Environ. Int. J. Devoted Catal. Sci. Its Appl.* **2019**, *251*, 119–129. [[CrossRef](#)]
51. Bell, F.A.T. In-Situ Infrared Study of Methanol Synthesis from H<sub>2</sub>/CO<sub>2</sub> over Cu/SiO<sub>2</sub> and Cu/ZrO<sub>2</sub>/SiO<sub>2</sub>. *J. Catal.* **1997**, *172*, 222–237.
52. Arena, F.; Italiano, G.; Barbera, K.; Bordiga, S.; Bonura, G.; Spadaro, L.; Frusteri, F. Solid-state interactions, adsorption sites and functionality of Cu-ZnO/ZrO<sub>2</sub> catalysts in the CO<sub>2</sub> hydrogenation to CH<sub>3</sub>OH. *Appl. Catal. A Gen.* **2008**, *350*, 16–23. [[CrossRef](#)]
53. Rodriguez, J.A.; Liu, P.; Graciani, J.; Senanayake, S.D.; Grinter, D.; Stacchiola, D.; Hrbek, J.; Fernandez Sanz, J. Inverse Oxide/Metal Catalysts in Fundamental Studies and Practical Applications: A Perspective of Recent Developments. *J. Phys. Chem. Lett.* **2016**, *7*, 2627–2639. [[CrossRef](#)]
54. Wu, C.; Lin, L.; Liu, J.; Zhang, J.; Ma, D. Inverse ZrO<sub>2</sub>/Cu as a highly efficient methanol synthesis catalyst from CO<sub>2</sub> hydrogenation. *Nat. Commun.* **2020**, *11*, 5767. [[CrossRef](#)]
55. Tisseraud, C.; Comminges, C.; Pronier, S.; Pouilloux, Y.; Valant, A.L. The Cu-ZnO synergy in methanol synthesis Part 3: Impact of the composition of a selective Cu@ZnOx core-shell catalyst on methanol rate explained by experimental studies and a concentric spheres model. *J. Catal.* **2016**, *343*, 106–114. [[CrossRef](#)]
56. Rui, N.; Zhang, F.; Sun, K.; Liu, Z.; Liu, C.J. Hydrogenation of CO<sub>2</sub> to Methanol on a Au<sup>δ+</sup>-In<sub>2</sub>O<sub>3-x</sub> Catalyst. *ACS Catal.* **2020**, *10*, 11307–11317. [[CrossRef](#)]
57. Koizumi, N.; Jiang, X.; Kugai, J.; Song, C. Effects of mesoporous silica supports and alkaline promoters on activity of Pd catalysts in CO<sub>2</sub> hydrogenation for methanol synthesis. *Catal. Today* **2012**, *194*, 16–24. [[CrossRef](#)]

58. Choi, E.J.; Lee, Y.H.; Lee, D.W.; Moon, D.J.; Lee, K.Y. Hydrogenation of CO<sub>2</sub> to methanol over Pd–Cu/CeO<sub>2</sub> catalysts. *Mol. Catal.* **2017**, *434*, 146–153. [[CrossRef](#)]
59. Vu, T.T.N.; Desgagnés, A.; Iliuta, M.C. Efficient approaches to overcome challenges in material development for conventional and intensified CO<sub>2</sub> catalytic hydrogenation to CO, methanol, and DME. *Appl. Catal. A Gen.* **2021**, *617*, 118119. [[CrossRef](#)]
60. Liu, P.N.; Rskov, J.K. Ligand and ensemble effects in adsorption on alloy surfaces. *Phys. Chem. Chem. Phys.* **2001**, *3*, 3814–3818. [[CrossRef](#)]
61. Liu, L.; Yao, H.; Jiang, Z.; Fang, T. Theoretical study of methanol synthesis from CO<sub>2</sub> hydrogenation on PdCu<sub>3</sub>(111) surface. *Appl. Surf. Sci. A J. Devoted Prop. Interfaces Relat. Synth. Behav. Mater.* **2018**, *451*, 333–345. [[CrossRef](#)]
62. Liu, L.; Fan, F.; Jiang, Z.; Gao, X.; Wei, J.; Fang, T. Mechanistic Study of Pd-Cu Bimetallic Catalysts for Methanol Synthesis from CO<sub>2</sub> Hydrogenation. *J. Phys. Chem. C* **2017**, *121*, 26287–26299. [[CrossRef](#)]
63. Qin, B.; Li, S. First principles investigation of dissociative adsorption of H<sub>2</sub> during CO<sub>2</sub> hydrogenation over cubic and hexagonal In<sub>2</sub>O<sub>3</sub> catalysts. *Phys. Chem. Chem. Phys.* **2020**, *22*, 3390–3399. [[CrossRef](#)]
64. Zhang, M.; Dou, M.; Yu, Y. Theoretical study of the promotional effect of ZrO<sub>2</sub> on In<sub>2</sub>O<sub>3</sub> catalyzed methanol synthesis from CO<sub>2</sub> hydrogenation. *Appl. Surf. Sci.* **2018**, *433*, 780–789. [[CrossRef](#)]
65. Ye, J.; Liu, C.; Ge, Q. DFT Study of CO<sub>2</sub> Adsorption and Hydrogenation on the In<sub>2</sub>O<sub>3</sub> Surface. *Am. Chem. Soc.* **2012**, *116*, 7817–7825. [[CrossRef](#)]
66. Ye, J.; Liu, C.J.; Mei, D.; Ge, Q. Active Oxygen Vacancy Site for Methanol Synthesis from CO<sub>2</sub> Hydrogenation on In<sub>2</sub>O<sub>3</sub>(110): A DFT Study. *ACS Catal.* **2013**, *3*, 1296–1306. [[CrossRef](#)]
67. Martin, O.; Pérez-Ramírez, J. New and revisited insights into the promotion of methanol synthesis catalysts by CO<sub>2</sub>. *Catal. Sci. Technol.* **2013**, *3*, 3343–3352. [[CrossRef](#)]
68. Dou, M.; Zhang, M.; Chen, Y.; Yu, Y. Theoretical study of methanol synthesis from CO<sub>2</sub> and CO hydrogenation on the surface of ZrO<sub>2</sub> supported In<sub>2</sub>O<sub>3</sub> catalyst. *Surf. Sci.* **2018**, *672*, 7–12. [[CrossRef](#)]
69. Shanshan, D.; Peng, G.; Ziyu, L.; Xinqing, C.; Chengguang, Y.; Hui, W.; Liangshu, Z.; Shenggang, L.; Yuhan, S. Role of zirconium in direct CO<sub>2</sub> hydrogenation to lower olefins on oxide/zeolite bifunctional catalysts. *J. Catal.* **2018**, *364*, 382–393.
70. Sharafutdinov, I.; Elkjær, C.F.; de Carvalho, H.W.P.; Gardini, D.; Chiarello, G.L.; Damsgaard, C.D.; Wagner, J.B.; Grunwaldt, J.D.; Dahl, S.; Chorkendorff, I. Intermetallic compounds of Ni and Ga as catalysts for the synthesis of methanol. *J. Catal.* **2014**, *320*, 77–88. [[CrossRef](#)]
71. Sha, F.; Han, Z.; Tang, S.; Wang, J.; Li, C. Hydrogenation of Carbon Dioxide to Methanol over Non-Cu-based Heterogeneous Catalysts. *ChemSusChem* **2020**, *13*, 6160–6181. [[CrossRef](#)] [[PubMed](#)]
72. Kakumoto, T.; Watanabe, T. A theoretical study for methanol synthesis by CO<sub>2</sub> hydrogenation. *Catal. Today* **1997**, *36*, 39–44. [[CrossRef](#)]
73. Kim, Y.; Trung, T.S.B.; Yang, S.; Kim, S.; Lee, H. Mechanism of the Surface Hydrogen Induced Conversion of CO<sub>2</sub> to Methanol at Cu(111) Step Sites. *ACS Catal.* **2016**, *6*, 1037–1044. [[CrossRef](#)]
74. Yang, Y.; Evans, J.; Rodriguez, J.A.; White, M.G.; Liu, P. Fundamental studies of methanol synthesis from CO<sub>2</sub> hydrogenation on Cu(111), Cu clusters, and Cu/ZnO(000). *Phys. Chem. Chem. Phys.* **2010**, *12*, 9909–9917. [[CrossRef](#)] [[PubMed](#)]
75. Larmier, K.; Liao, W.C.; Tada, S.; Lam, E.; Verel, D.R.; Bansode, A.; Urakawa, A.; Comas-Vives, A.; Copéret, P.C. CO<sub>2</sub>-to-Methanol Hydrogenation on Zirconia-Supported Copper Nanoparticles: Reaction Intermediates and the Role of the Metal-Support Interface. *Angew. Chem.* **2017**, *56*, 2318–2323. [[CrossRef](#)] [[PubMed](#)]
76. Gao, P.; Li, S.; Bu, X.; Dang, S.; Liu, Z.; Wang, H.; Zhong, L.; Qiu, M.; Yang, C.; Cai, J. Direct conversion of CO<sub>2</sub> into liquid fuels with high selectivity over a bifunctional catalyst. *Nat. Chem.* **2017**, *9*, 1019–1024. [[CrossRef](#)]
77. Grabow, L.C.; Mavrikakis, M. Mechanism of Methanol Synthesis on Cu through CO<sub>2</sub> and CO Hydrogenation. *ACS Catal.* **2011**, *1*, 365–384. [[CrossRef](#)]
78. Nie, X.; Jiang, X.; Wang, H.; Luo, W.; Janik, M.J.; Chen, Y.; Song, C. Mechanistic Understanding of Alloy Effect and Water Promotion for Pd-Cu Bimetallic Catalysts in CO<sub>2</sub> Hydrogenation to Methanol. *ACS Catal.* **2018**, *8*, 4873–4892. [[CrossRef](#)]
79. Zhang, M.; Dou, M.; Yu, Y. DFT study of CO<sub>2</sub> conversion on InZr<sub>3</sub>(110) surface. *Phys. Chem. Chem. Phys. PCCP* **2017**, *19*, 28917–28927. [[CrossRef](#)]
80. Yang, Y.; White, M.G.; Liu, P. Theoretical Study of Methanol Synthesis from CO<sub>2</sub> Hydrogenation on Metal-Doped Cu(111) Surfaces. *J. Phys. Chem. C* **2012**, *116*, 248–256. [[CrossRef](#)]
81. Liu, L.; Fan, F.; Bai, M.; Xue, F.; Ma, X.; Jiang, Z.; Fang, T. Mechanistic study of methanol synthesis from CO<sub>2</sub> hydrogenation on Rh-doped Cu(111) surfaces. *Mol. Catal.* **2019**, *466*, 26–36. [[CrossRef](#)]
82. Kattel, S.; Yan, B.; Yang, Y.; Chen, J.G.; Liu, P. Optimizing Binding Energies of Key Intermediates for CO<sub>2</sub> Hydrogenation to Methanol over Oxide-Supported Copper. *J. Am. Chem. Soc.* **2016**, *138*, 12440. [[CrossRef](#)] [[PubMed](#)]
83. Tang, Q.L.; Hong, Q.J.; Liu, Z.P. CO<sub>2</sub> fixation into methanol at Cu/ZrO<sub>2</sub> interface from first principles kinetic Monte Carlo. *J. Catal.* **2009**, *263*, 114–122. [[CrossRef](#)]
84. Yang, Y.; Mei, D.; Peden, C.H.F.; Campbell, C.T.; Mims, C.A. Surface-Bound Intermediates in Low-Temperature Methanol Synthesis on Copper: Participants and Spectators. *ACS Catal.* **2015**, *5*, 7328–7337. [[CrossRef](#)]
85. Zhao, Y.-F.; Yang, Y.; Mims, C.; Peden, C.H.F.; Li, J.; Mei, D. Insight into methanol synthesis from CO<sub>2</sub> hydrogenation on Cu(111): Complex reaction network and the effects of H<sub>2</sub>O. *J. Catal.* **2011**, *281*, 199–211. [[CrossRef](#)]

86. Tang, Q.; Shen, Z.; Russell, C.K.; Fan, M. Thermodynamic and Kinetic Study on Carbon Dioxide Hydrogenation to Methanol over a Ga<sub>3</sub>Ni<sub>5</sub>(111) Surface: The Effects of Step Edge. *J. Phys. Chem. C. Nanomater. Interfaces* **2018**, *122*, 315–330. [[CrossRef](#)]
87. Tang, Q.; Shen, Z.; Huang, L.; He, T.; Fan, M. Synthesis of methanol from CO<sub>2</sub> hydrogenation promoted by dissociative adsorption of hydrogen on a Ga<sub>3</sub>Ni<sub>5</sub>(221) surface. *Phys. Chem. Chem. Phys. PCCP* **2017**, *19*, 18539–18555. [[CrossRef](#)]
88. Chinchin, G.C.; Waugh, K.C.; Whan, D.A. The activity and state of the copper surface in methanol synthesis catalysts. *Appl. Catal.* **1986**, *25*, 101–107. [[CrossRef](#)]
89. Liu, X.M.; Lu, G.Q.; Yan, Z.F.; Beltramini, J. Recent advances in catalysts for methanol synthesis via hydrogenation of CO and CO<sub>2</sub>. *Ind. Eng. Chem. Res.* **2003**, *42*, 6518–6530. [[CrossRef](#)]
90. Pan, W.X.; Cao, R.; Roberts, D.L.; Griffin, G.L. Methanol synthesis activity of Cu/ZnO catalysts. *Cheminform* **1989**, *2*, 440–446. [[CrossRef](#)]
91. Chorkendorff, P.B.R.K. Synthesis of methanol from a mixture of H<sub>2</sub> and CO<sub>2</sub> on Cu(100). *Surf. Sci.* **1994**, *318*, 267–280.
92. Askgaard, T.S.; Norskov, J.K.; Ovesen, C.V.; Stoltze, P. A Kinetic Model of Methanol Synthesis. *J. Catal.* **1995**, *156*, 229–242. [[CrossRef](#)]
93. Karelovic, A.; Bargibant, A.; Fernández, C.; Ruiz, P. Effect of the structural and morphological properties of Cu/ZnO catalysts prepared by citrate method on their activity toward methanol synthesis from CO<sub>2</sub> and H<sub>2</sub> under mild reaction conditions. *Catal. Today* **2012**, *197*, 109–118. [[CrossRef](#)]
94. Clausen, B.S.; Steffensen, G.; Fabius, B.; Villadsen, J.; Feidenhans' L, R.; TopsøE, H. In situ cell for combined XRD and on-line catalysis tests: Studies of Cu-based water gas shift and methanol catalysts. *J. Catal.* **1991**, *132*, 524–535. [[CrossRef](#)]
95. Liu, J.; Shi, J.; He, D.; Zhang, Q.; Wu, X.; Liang, Y.; Zhu, Q. Surface active structure of ultra-fine Cu/ZrO<sub>2</sub> catalysts used for the CO<sub>2</sub>+H<sub>2</sub> to methanol reaction. *Appl. Catal. A Gen.* **2001**, *218*, 113–119. [[CrossRef](#)]
96. Herman, R.G.; Klier, K.; Simmons, G.W.; Finn, B.P.; Bulko, J.B.; Kobylinski, T.P. Catalytic synthesis of methanol from CO/H<sub>2</sub>I. Phase composition, electronic properties, and activities of the Cu/ZnO/M<sub>2</sub>O<sub>3</sub> catalysts. *J. Catal.* **1979**, *56*, 407–429. [[CrossRef](#)]
97. Szanyi, J.; Goodman, D.W. Methanol synthesis on a Cu(100) catalyst. *Catal. Lett.* **1991**, *10*, 383–390. [[CrossRef](#)]
98. Jedrecy, N.; Gallini, S.; Sauvage-Simkin, M.; Pinchaux, R. Copper growth on the O-terminated ZnO (0001) surface: Structure and morphology. *Phys. Rev. B* **2001**, *64*, 085424. [[CrossRef](#)]
99. Arena, F.; Di Chio, R.; Filiciotto, L.; Trunfio, G.; Espro, C.; Palella, A.; Patti, A.; Spadaro, L. Probing the functionality of nanostructured MnCeO<sub>x</sub> catalysts in the carbon monoxide oxidation Part II. Reaction mechanism and kinetic modelling. *Appl. Catal. B Environ.* **2017**, *218*, 803–809. [[CrossRef](#)]
100. Li, L.J.G.F. Influence of copper content on structural features and performance of pre-reduced LaMn<sub>1-x</sub>Cu<sub>x</sub>O<sub>3</sub> (0 ≤ x < 1) catalysts for methanol synthesis from CO<sub>2</sub>/H<sub>2</sub>. *J. Rare Earths* **2010**, *25*, 747–751.
101. Nakamura, J.; Uchijima, T.; Kanai, Y.; Fujitani, T. The role of ZnO in Cu/ZnO methanol synthesis catalysts. *Catal. Today* **1996**, *28*, 223–230. [[CrossRef](#)]
102. Arena, F.; Italiano, G.; Barbera, K.; Bonura, G.; Spadaro, L.; Frusteri, F. Basic evidences for methanol-synthesis catalyst design. *Catal. Today* **2009**, *143*, 80–85. [[CrossRef](#)]
103. Kasatkin, I.; Kurr, P.; Kniep, B.; Trunschke, A.; Schlögl, R. Role of Lattice Strain and Defects in Copper Particles on the Activity of Cu/ZnO/Al<sub>2</sub>O<sub>3</sub> Catalysts for Methanol Synthesis. *Angew. Chem. Int. Ed.* **2007**, *46*, 7324–7327. [[CrossRef](#)] [[PubMed](#)]
104. Behrens, M. Meso- and nano-structuring of industrial Cu/ZnO/(Al<sub>2</sub>O<sub>3</sub>) catalysts. *J. Catal.* **2009**, *267*, 24–29. [[CrossRef](#)]
105. Mehta, S.; Simmons, G.W.; Klier, K.; Herman, R.G. Catalytic synthesis of methanol from ja:math: II. Electron microscopy (TEM, STEM, microdiffraction, and energy dispersive analysis) of the ja:math and Cu/ZnO/Cr<sub>2</sub>O<sub>3</sub> catalysts. *J. Catal.* **1979**, *57*, 339–360. [[CrossRef](#)]
106. Natesakhawat, S.; Lekse, J.W.; Baltrus, J.P.; Ohodnicki, P.R.; Howard, B.H.; Deng, X.; Matranga, C. Active Sites and Structure–Activity Relationships of Copper-Based Catalysts for Carbon Dioxide Hydrogenation to Methanol. *Acs Catal.* **2012**, *2*, 1667–1676. [[CrossRef](#)]
107. Oguchi, H.; Kanai, H.; Utani, K.; Matsumura, Y.; Imamura, S. Cu<sub>2</sub>O as active species in the steam reforming of methanol by CuO/ZrO<sub>2</sub> catalysts. *Appl. Catal. A Gen.* **2005**, *293*, 64–70. [[CrossRef](#)]
108. Liao, F.; Huang, Y.; Ge, J.; Zheng, W.; Tedsree, K.; Collier, P.; Hong, X.; Tsang, S.C. Morphology-Dependent Interactions of ZnO with Cu Nanoparticles at the Materials' Interface in Selective Hydrogenation of CO<sub>2</sub> to CH<sub>3</sub>OH. *Angew. Chem. Int. Ed.* **2011**, *50*, 2162–2165. [[CrossRef](#)]
109. Melián-Cabrera, I.; Granados, M.L.; Fierro, J.L.G. Pd-Modified Cu–Zn Catalysts for Methanol Synthesis from CO<sub>2</sub>/H<sub>2</sub> Mixtures: Catalytic Structures and Performance. *J. Catal.* **2002**, *210*, 285–294. [[CrossRef](#)]
110. Zhang, Q.X.Z.; Qian, Z.H. Synthesis of methanol from CO<sub>2</sub>/H<sub>2</sub> at low pressure on CuO-ZnO and CuO-ZnO-ZrO<sub>2</sub> catalysts. *J. Catal.* **1989**, *10*, 22–28.
111. Kanai, Y.; Watanabe, T.; Fujitani, T.; Uchijima, T.; Nakamura, J. The synergy between Cu and ZnO in methanol synthesis catalysts. *Catal. Lett.* **1996**, *38*, 157–163. [[CrossRef](#)]
112. Grunwaldt, J.D.; Molenbroek, A.M.; Topse, N.Y.; Topse, H.; Clausen, B.S. In Situ Investigations of Structural Changes in Cu/ZnO Catalysts. *J. Catal.* **2000**, *194*, 452–460. [[CrossRef](#)]
113. Behrens, M.; Studt, F.; Kasatkin, I.; Kuehl, S.; Haevecker, M.; Abild-Pedersen, F.; Zander, S.; Girgsdies, F.; Kurr, P.; Kniep, B.-L.; et al. The Active Site of Methanol Synthesis over Cu/ZnO/Al<sub>2</sub>O<sub>3</sub> Industrial Catalysts. *Science* **2012**, *336*, 893–897. [[CrossRef](#)] [[PubMed](#)]

114. Kurtz, M.; Strunk, J.; Hinrichsen, O.; Muhler, M.; Fink, K.; Meyer, B.; Wöll, C. Active Sites on Oxide Surfaces: ZnO-Catalyzed Synthesis of Methanol from CO and H<sub>2</sub>. *Angew. Chem. Int. Ed.* **2005**, *44*, 2790–2794. [[CrossRef](#)] [[PubMed](#)]
115. Le Valant, A.; Comminges, C.; Tisseraud, C.; Canaff, C.; Pinard, L.; Pouilloux, Y. The Cu-ZnO synergy in methanol synthesis from CO<sub>2</sub>, Part 1: Origin of active site explained by experimental studies and a sphere contact quantification model on Cu plus ZnO mechanical mixtures. *J. Catal.* **2015**, *324*, 41–49. [[CrossRef](#)]
116. Kattel, S.; Ramírez, P.J.; Chen, J.G.; Rodriguez, J.A.; Liu, P. Active sites for CO<sub>2</sub> hydrogenation to methanol on Cu/ZnO catalysts. *Science* **2017**, *355*, 1296–1299. [[CrossRef](#)] [[PubMed](#)]
117. Habraken, F.H.P.M.; Mesters, C.M.A.M.; Bootsma, G.A. The adsorption and incorporation of oxygen on Cu (100) and its reaction with carbon monoxide; comparison with Cu (111) and Cu (110). *Surf. Sci.* **1980**, *97*, 264–282. [[CrossRef](#)]
118. Norton, P.R.; Tapping, R.L. Photoelectron spectroscopic studies of the adsorption of CO and CO<sub>2</sub> on nickel, platinum and copper. *Chem. Phys. Lett.* **1976**, *38*, 207–212. [[CrossRef](#)]
119. Chinchin, G.C.; Spencer, M.S.; Waugh, K.C.; Whan, D.A. Promotion of methanol synthesis and the water-gas shift reactions by adsorbed oxygen on supported copper catalysts. *J. Chem. Soc. Faraday Trans. Phys. Chem. Condens. Phases* **1987**, *83*, 2193–2212. [[CrossRef](#)]
120. Wachs, I.E.; Madix, R.J. Selective oxidation of CH<sub>3</sub>OH to H<sub>2</sub>CO on a copper(110) catalyst. *J. Catal.* **1978**, *53*, 208–227. [[CrossRef](#)]
121. Hadden, R.A.; Vandervell, H.D.; Waugh, K.C.; Webb, G. The adsorption and decomposition of carbon dioxide on polycrystalline copper. *Catal. Lett.* **1988**, *1*, 27–33. [[CrossRef](#)]
122. Sakakini, B.H.; Tabatabaei, J.; Watson, M.J.; Waugh, K.C. Structural changes of the Cu surface of a Cu/ZnO/Al<sub>2</sub>O<sub>3</sub> catalyst, resulting from oxidation and reduction, probed by CO infrared spectroscopy. *J. Mol. Catal. A Chem.* **2000**, *162*, 297–306. [[CrossRef](#)]
123. Copperthwaite, R.G.; Davies, P.R.; Morris, M.A.; Roberts, M.W.; Ryder, R.A. The reactive chemisorption of carbon dioxide at magnesium and copper surfaces at low temperature. *Catal. Lett.* **1988**, *1*, 11–19. [[CrossRef](#)]
124. Rodriguez, J.A.; Liu, P.; Stacchiola, D.; Senanayake, S.D.; White, M.G.; Chen, J.G. Hydrogenation of CO<sub>2</sub> to Methanol: Importance of Metal-Oxide and Metal-Carbide Interfaces in the Activation of CO<sub>2</sub>. *ACS Catal.* **2015**, *5*, 6696–6706. [[CrossRef](#)]
125. Burch, R.; Golunski, S.E.; Spencer, M.S. The role of copper and zinc oxide in methanol synthesis catalysts. *J. Chem. Soc. Faraday Trans.* **1990**, *86*, 2683–2691. [[CrossRef](#)]
126. Auroux, A.; Gervasini, A. Microcalorimetric Study of the Acidity and Basicity of Metal Oxide Surfaces. *Cheminform* **1990**, *21*, 4. [[CrossRef](#)]
127. Bianchi, D.; Chafik, T.; Khalfallah, M.; Teichner, S.J. Intermediate species on zirconia supported methanol aerogel catalysts: IV. Adsorption of carbon dioxide. *Appl. Catal. A Gen.* **1994**, *112*, 219–235. [[CrossRef](#)]

**Disclaimer/Publisher’s Note:** The statements, opinions and data contained in all publications are solely those of the individual author(s) and contributor(s) and not of MDPI and/or the editor(s). MDPI and/or the editor(s) disclaim responsibility for any injury to people or property resulting from any ideas, methods, instructions or products referred to in the content.